ADVANCED MATERIALS
www.advmat.de

Origami and Kirigami on Nanomembranes: Design, Fabrication, and Applications

Xiang Dong, Xing Li, Jizhai Cui, and Yongfeng Mei**

Origami and kirigami, traditional arts that transform flat sheets into intricate three-dimensional structures through the design of creases and cuts, have inspired a wide range of engineering applications across multiple fields. These scale-independent fabrication techniques have been adapted to nanomembranes, enabling the construction of reconfigurable micro- and nanostructures with unique properties that are challenging to achieve through conventional methods. This review highlights recent advancements in the design, fabrication, and applications of origami and kirigami on nanomembranes. Fundamental design theories for crease and cut patterns on nanomembranes and their corresponding mechanical responses under large deformations, such as twisting and bending, are discussed together with the actuation mechanisms that facilitate the transition from two-dimensional patterns to three-dimensional structures. Recently developed microfabrication methods are summarized, including patterning, detachment, and transfer printing for nanomembranes. The applications of nanomembrane-based origami and kirigami devices in optoelectronics, micro/nanorobots, and metamaterials are highlighted, which take advantage of the reconfigurable complex 3D microstructures. Key challenges in the field are identified, and future research directions are proposed to further integrate origami and kirigami principles into nanomembrane engineering. This overview aims to provide researchers with a comprehensive reference to foster further innovations and applications in this emerging interdisciplinary domain.

1. Introduction

Origami (paper folding) and kirigami (paper cutting) are ancient arts of transforming flat sheets into three-dimensional (3D) shapes.[1] In modern materials science, these purely geometric techniques provide a scale-independent framework for creating 3D architectures[2–4] from thin two-dimensional (2D) films, or nanomembranes. A nanomembrane is a freestanding or transferable thin film that is often only a few nanometers to hundreds of nanometers thick, exhibiting high flexibility.[5] By applying origami and kirigami design rules to such nanomembranes, engineers can achieve 2D-to-3D geometrical transformations that were previously impossible with rigid, thicker materials.[6–9] The folding and cutting methods have also been adapted to diverse functional materials, ranging from single-crystal silicon,[10] oxides,[11] to polymers[12,13] and graphene.[14] The resulting 3D micro/nanostructures with feature sizes from tens of nanometers to millimeters can host unique properties distinct from bulk materials, giving rise to new functionalities in electronics,[15] optics,[16,17] magnetics,[18] mechanics,[19] and beyond.

The motivation for origami/kirigami-based 3D assembly is the promise of enhanced or novel functionalities that 3D geometries can provide. For example, folding 2D nanomembranes[5,14,20,21] into 3D shapes[22–25] can achieve optoelectronic devices with improved light capture and field of view,[24,26] metamaterials with exotic electromagnetic behavior,[27,28] and microscale robots,[29–32] as illustrated in **Figure 1**. However, a major challenge in realizing such systems is the lack of fabrication/assembly methods that offer both the necessary resolution (micro/nanoscale features) and the required materials compatibility. Traditional 3D printing or multiphoton lithography[33,34] can produce high-resolution structures but cannot directly use semiconductor-grade thin films. On the other hand, self-folding strategies using special materials (e.g., shape memory polymers[35] or hydrogels[36]) achieve 3D shapes but often sacrifice material performance (not suitable for electronics) or geometric versatility. The origami/kirigami paradigm addresses these gaps by leveraging standard planar microfabrication of a large variety of thin films, followed by out-of-plane transformation to create 3D structures.

Still, significant challenges remain in this emerging field: the mechanics of nanoscale folding can differ from macroscale paper folding, fabrication methods must balance precision with scalability, and integrating these delicate 3D structures into functional devices is non-trivial. This timely review provides a

X. Dong, X. Li, J. Cui, Y. Mei
International Institute for Intelligent Nanorobots and Nanosystems & State Key Laboratory of Surface Physics
College of Intelligent Robotics and Advanced Manufacturing
Fudan University
Shanghai 200438, P. R. China
E-mail: jzcui@fudan.edu.cn; yfm@fudan.edu.cn

Y. Mei
Yiwu Research Institute of Fudan University
Yiwu, Zhejiang 322000, P. R. China

Y. Mei
Shanghai Frontiers Science Research Base of Intelligent Optoelectronics and Perception
Institute of Optoelectronics
Fudan University
Shanghai 200438, P. R. China

The ORCID identification number(s) for the author(s) of this article can be found under https://doi.org/10.1002/adma.202510883

DOI: 10.1002/adma.202510883

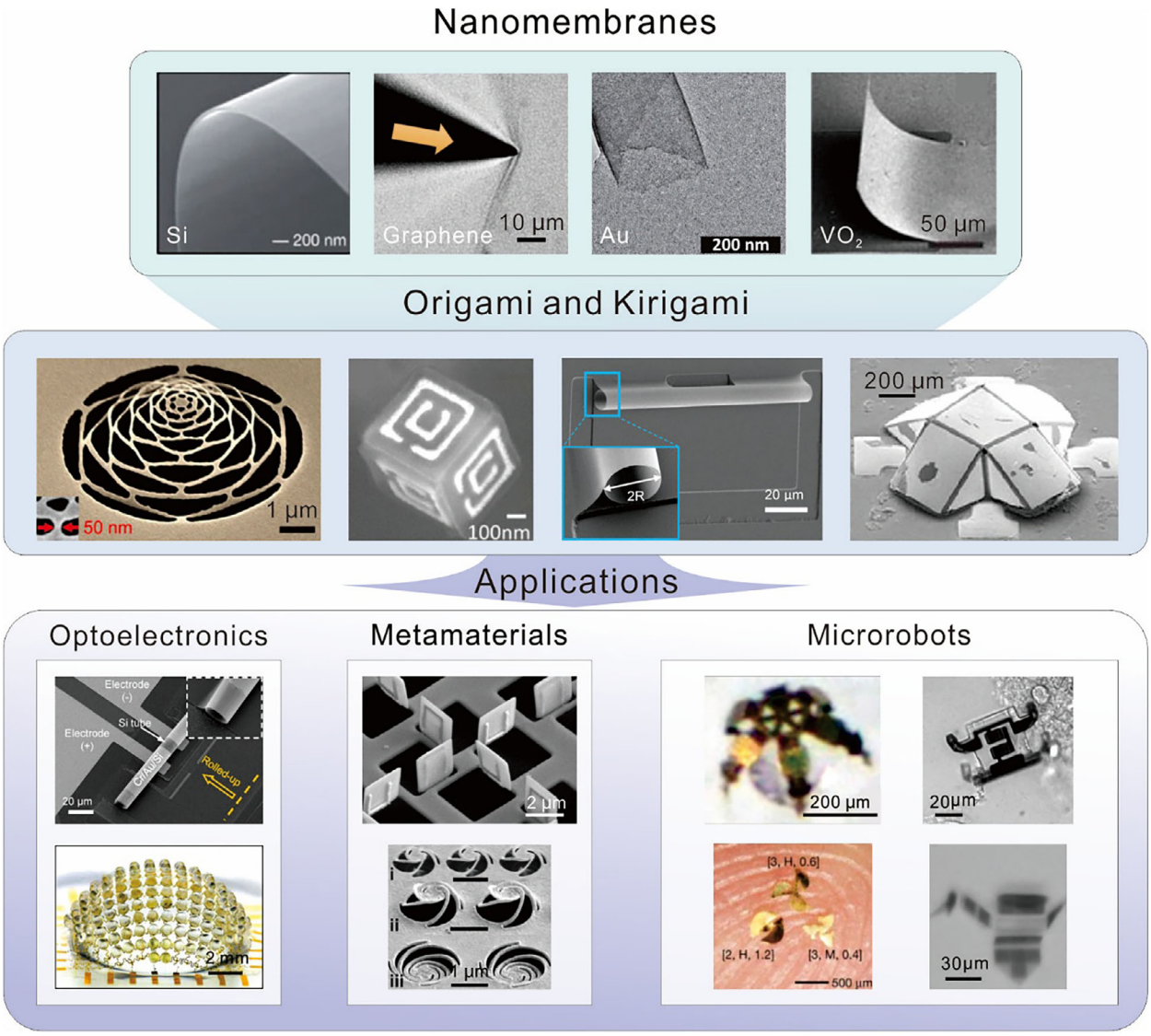

Figure 1. An overview of the nanomembranes implemented with origami and kirigami concepts to achieve 2D-to-3D transformation for advanced functionalities in optoelectronics, metamaterials, and microrobots.[5,14,20–32] Top panel: silicon, graphene, Au, and VO_2 nanomembranes. Adapted with permission.[5,14,20,21] Left to right: Copyright 2011, Springer Nature; Copyright 2015, Springer Nature; Copyright 2015, American Chemical Society (ACS); Copyright 2019, Institute of Physics (IOP). Middle panel: 3D microdome, Al_2O_3 folded cubes, Si tube, and bilayer of Au and SU8 origami. Adapted with permission.[22–25] Left to right: Copyright 2018, American Association for the Advancement of Science (AAAS); Copyright 2011, Wiley; Copyright 2023, Wiley; Copyright 2016, Wiley. Bottom panel: optoelectronics (polarization photodetector and digital camera), metamaterials (folded 3D metamaterials and nano-electromechanical system), and microrobots (microgripper, microwalker, microflier and microscale "bird"). Adapted with permission.[24,26–32] Optoelectronics, top to bottom: Copyright 2023, Wiley; Copyright 2013, Springer Nature. Metamaterials, top to bottom: Copyright 2017, Wiley; Copyright 2021, Springer Nature. Microrobots: top left. Copyright 2008, ACS; top right, copyright 2020, Springer Nature; bottom left, Copyright 2021, Springer Nature; bottom right, Copyright 2019, Springer Nature.

comprehensive overview of the state of the art in origami and kirigami applied to nanomembranes. In the sections that follow, we discuss the theoretical design principles, the mechanical behavior of thin films during folding, and the physical actuation mechanisms enabling 2D-to-3D shape changes. We then survey fabrication strategies for patterning, releasing, and integrating origami/kirigami nanomembranes. Finally, we highlight a range of device applications, including optoelectronics, transformable microrobots, and reconfigurable metamaterials, and we conclude with an outlook on current challenges and future prospects in order to inform and inspire further research in this exciting interdisciplinary domain.

2. Design Theory

2.1. Origami and Kirigami Fundamentals

In origami engineering, a flat sheet is transformed into a target 3D shape purely by folding along prescribed lines (creases) without cutting the material.[2] Kirigami introduces cuts or voids

in the sheet, which provides additional degrees of freedom for deformation. Both techniques are inherently scalable: the same geometric principles apply from the macroscale (paper models) down to the microscale. The classical origami model treats the sheet as an ideal thin, inextensible surface that bends at zero-thickness crease lines.[3] This model works well when the material is sufficiently thin and flexible, as is the case for many nanomembranes. However, real materials have finite thickness and may not accommodate sharp folds easily. Kirigami alleviates some of these limitations by removing material (through cuts or slits) to release strain and allow motions that pure bending cannot achieve.[4] A simple example is a flat ribbon with periodic cuts that can stretch like a spring; at the nanoscale, this concept was applied to one-atom-thick graphene, where kirigami cuts enabled the graphene to act as a robust, flexible spring that could be stretched by ~70% without breaking.[14] In that groundbreaking demonstration of graphene kirigami, the cuts and resulting hinges allowed a normally rigid 2D material to behave like an elastic membrane, highlighting the power of kirigami design even at atomic thickness.

The design of origami/kirigami patterns for nanomembranes draws on both artistic intuition and mathematical theory. Origami patterns are often defined by crease graphs (networks of mountain and valley folds) that satisfy geometric constraints to be physically foldable. For instance, flat-foldability is a crucial property in origami design, as it determines whether the entire structure can always be transformed into a flat, planar shape during the folding process.[2] This property ensures that the origami model can be completely flattened without any distortions or overlaps, which is critical for applications on nanomembranes made by planar microfabrication techniques.[7] Kawasaki's theorem provides a criterion for determining whether a crease pattern with a single vertex can be folded into a flat shape. The theorem states that such a pattern is flat-foldable if and only if the alternating sum of the angles of consecutive folds around the vertex equals zero, ensuring that the pattern can be folded without any overlaps or gaps.[37,38] Many flat-foldable origami patterns have been developed, including the Miura-ori,[39] Eggbox,[40] Blockfold,[41] and many with rotational symmetry[42] (**Figure 2a**). Varying the design parameters of these patterns lead to highly tunable mechanical properties, including Poisson's ratio,[39,43] anisotropic stiffness,[44,45] and multistability,[46–48] which benefits the design of nanomembranes for reconfigurable 3D micro/nanostructures.

Kirigami patterns are defined by cut geometries in addition to folds; strategic placement of cuts can transform a brittle film into a compliant mesh capable of large out-of-plane displacement. Kirigami transformation can be achieved by structural buckling or rotating units.[4] Once a flat sheet is perforated with cuts, the effective modulus of the structure is significantly lowered compared to its intact form, and could be anisotropic. The out-of-plane deformation may exhibit significantly lower stiffness compared to the in-plane deformation, exhibiting out-of-plane buckling under in-plane mechanical loading and forming 3D structures[6,14,49] (Figure 2b). By rationally designing the cuts, one could also achieve a kirigami structure with a collection of rotating units under stretching.[50] In this case, the rotating units are considered as rigid panels linked by rotational hinges at corners. In practical designs, this may lead to high stress concentrations at the hinges and limit the degrees of freedom of the deformation. A design with out-of-plane foldable hinges is a possible way to release such constrains[51,52] (Figure 2c). This type of transformation combines the kirigami concept with cuts together with the origami concept with folding, leading to a wide design space for complex 3D structures that are previously unattainable, including morphing between flat sheets and closed surfaces[53,54] (Figure 2d).

Artificial intelligence (AI) algorithms are becoming essential for origami/kirigami inverse design because the pattern spaces are combinatorial, while forward evaluations are costly. Early work used model-based offline reinforcement learning: an emulator based on a convolutional neural network (CNN) and trained on molecular dynamics (MD) data, guided a sequential cut-placement policy to maximize stretchability in MoS_2 kirigami, mitigating the prohibitive ~6-h-per-structure simulation burden during search.[55] As the field shifted toward reproducing prescribed 3D shapes, inverse-design frameworks posed surface approximation as a two-stage optimization over rigid, flat-foldable quadrilateral-mesh origami, ensuring deployability while handling nonconvex constraints and demonstrating both smooth curvatures and sharp ridges.[56] Extending beyond 2D surfaces, a volumetric inverse-design approach for curvilinear modular origami mapped unit cells into target 3D geometries and then explored geometric/topological combinations to achieve the desired mobility, highlighting the need for AI-assisted exploration of vast design spaces.[57] Most recently, a purely geometric strategy for kirigami inverse design programs morphing by tuning rotating-unit shapes and without relying on large-scale numerical solvers; such rule-based insights are complementary to AI, which can prioritize feasible patterns and trade off multi-objective criteria (shape fidelity, deployability, actuation).[58] In sum, combining AI-driven global search with geometry-based priors yields an interpretable, closed-loop pipeline for inverse-designing deployable and non-developable origami/kirigami with coupled multiphysics performance.

Recent studies demonstrate that both origami and kirigami principles, including conformability, multistability, and the ability to induce large deformations, are not only preserved but also enhanced when applied to nanomembranes. Silverberg et al. demonstrated that origami structures at the microscale exhibit bistability, where hidden degrees of freedom in crease patterns allow for transitions between stable configurations, preserving multistability even at the nanoscale.[13] Zhu et al. introduced an electrothermal micro-origami system that enables rapid and reversible elastic folding, as well as plastic folding for reprogramming static shapes, preserving the conformal properties of origami at the microscale[59] (Figure 2e). Song et al. applied origami principles to silicon nanomembranes, creating reconfigurable 3D structures that maintained the conformability and tunable mechanical properties of origami.[60] Rao et al. developed kirigami-based stretchable imagers, using a design that enabled high stretchability while maintaining a high pixel fill factor,[61] as shown in Figure 2f. The imager, made of ultrathin silicon optoelectronic pixel arrays, could stretch biaxially by 30% without losing its electrical performance. Blees et al. showed that kirigami applied to graphene allowed the material to act as a stretchable spring, preserving the key properties of kirigami (such as flexibility and resilience) at the atomic scale[14] (Figure 2g). The

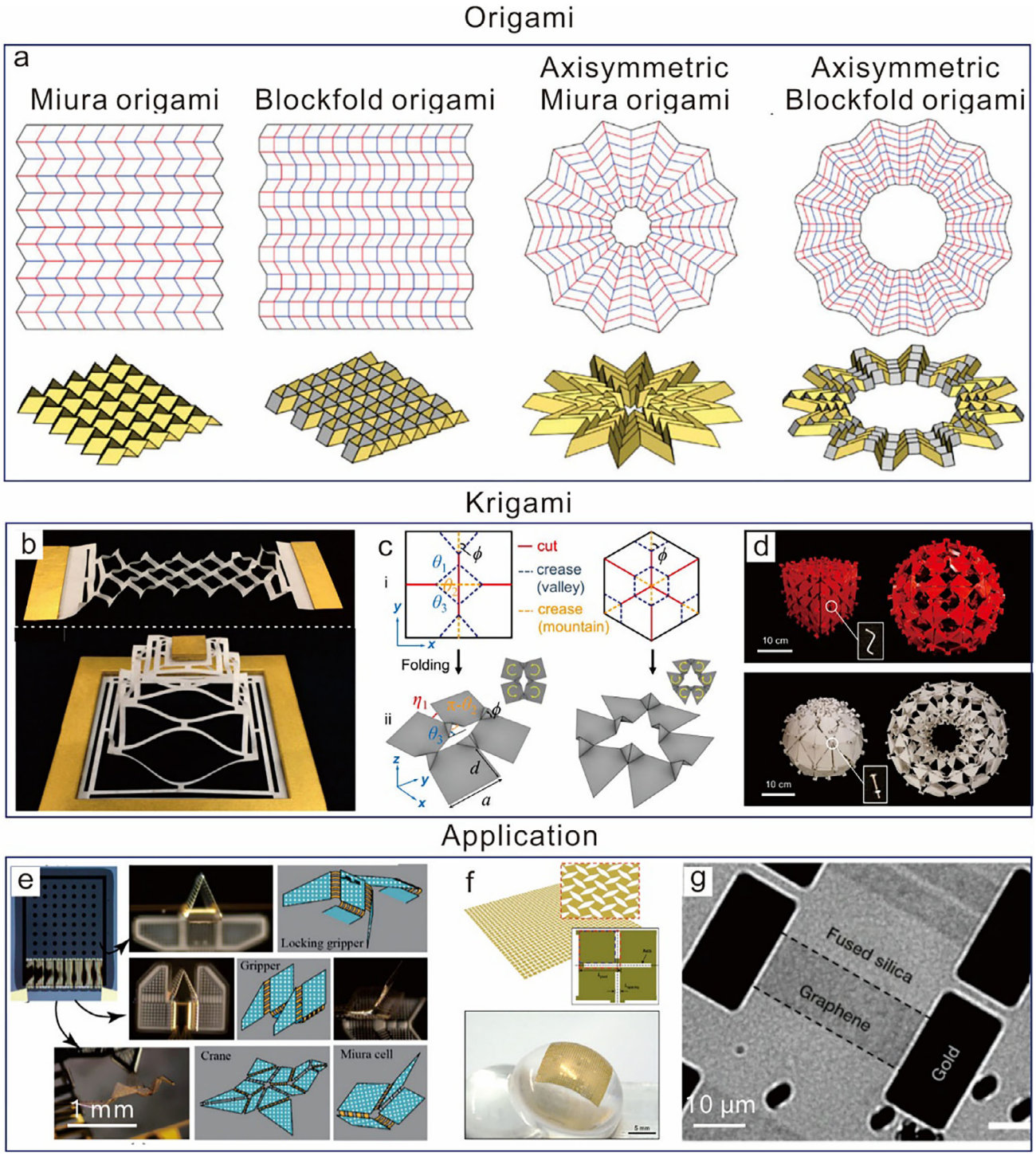

Figure 2. Origami and kirigami fundamentals. a) The crease patterns and folded configurations of Miura origami, Blockfold origami, axisymmetric Miura origami, and axisymmetric blockfold origami. Adapted with permission.[41] Copyright 2024, the Royal Society. b) Paper kirigami springs. Adapted with permission.[14] Copyright 2015, Springer Nature. c) Two-dimensional reconfigurable kirigami metasheets constructed from combined cuts and folds. Reproduced with permission.[51] Copyright 2019, National Academy of Sciences. d) 3D printed shape-morphing ori–kiri assemblage: compact cube or sphere (left) and deployed sphere (right). Reproduced with permission.[54] Copyright 2025, AAAS. e) The fabrication method can simultaneously fabricate various micro-origami with different geometries and functions on the same wafer. Adapted with permission.[59] Copyright 2020, Wiley. f) Schematic of a biaxially stretched kirigami sheet and an optical image of the bilayer device on a hemispherical polydimethylsiloxane (PDMS) surface after conformal additive stamp (CAS) printing. Inset: an enlarged view of the stretched kirigami sheet and the geometry of a repeating kirigami unit showing the pixel and space regions. Reproduced with permission.[61] Copyright 2021, Springer Natrue. g) Manipulating devices with a large sheet of graphene and gold pads. Adapted with permission.[14] Copyright 2015, Springer Nature.

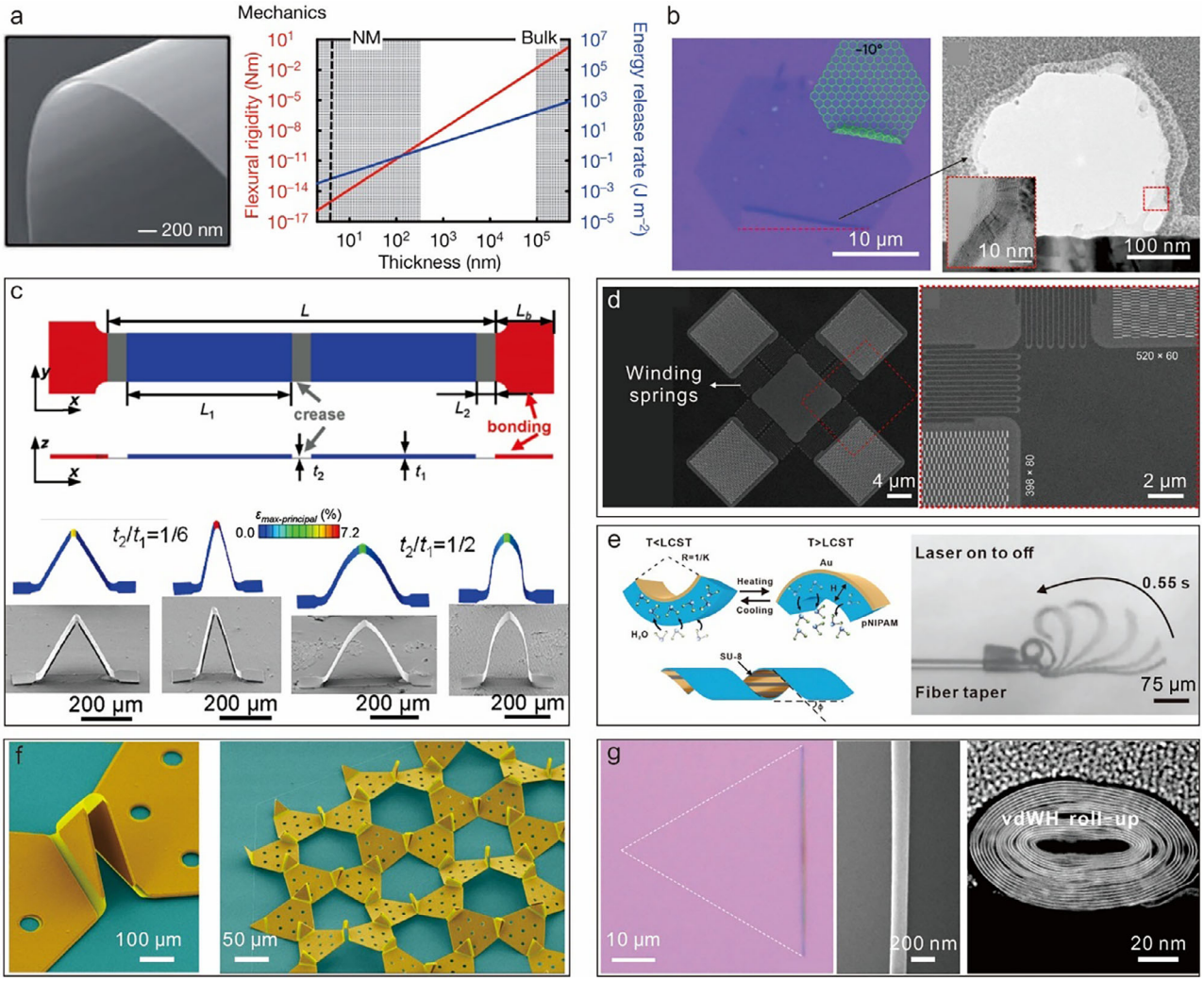

Figure 3. Mechanical behaviors of nanomembranes during the folding process. a) The scanning electron microscope (SEM) image of the Si nanomembrane and the curves of bending stiffness and energy release rate vary with the thickness of the Si nanomembrane. Reproduced with permission.[5] Copyright 2011, Springer Nature. b) Optical microscopy images of spontaneous rolling along the zigzag edge at −10° and cross-sectional Transmission Electron Microscope (TEM) image of a representative multi-walled graphene roll. Higher-resolution cross-sectional TEM image of the area marked in the red zone. Reproduced with permission.[47] Copyright 2025, Springer Nature. c) Top and cross-sectional views of a straight ribbon with two different thicknesses and a fixed length ratio ($L_2/L = 0.05$) and two different thickness ratios (t_2/t_1). Adapted with permission.[25] Copyright 2016, Wiley. d) SEM images of a four-panel micromachine. Adapted with permission.[32] Copyright 2019, Springer Nature. e) Schematic of deformation of pNIPAM/Au bilayer heterostructures induced by diffusion of H_2O molecules, and schematic of the actuation of a frog's tongue and optical image of a waveguide microactuator. Reproduced (Adapted) with permission. Reproduced with permission.[64] Copyright 2025, Wiley. f) A false-colored SEM image of a microsplay hinge and a metabot sheet. Here, the surface electrochemical actuators (SEAs) appear bright yellow, and the panels are colored orange. Reproduced with permission.[65] Copyright 2025, Springer Nature. g) Optical microscopy images and SEM image of a SnS_2/WSe_2 roll-up. Adapted with permission.[66] Copyright 2021, Springer Nature.

successful translation of these properties to the microscale and nanoscale emphasizes the scalability of these techniques and their potential for advancing reconfigurable nanostructures in a variety of applications.

2.2. Mechanical Behaviors of Nanomembranes during the Folding Process

When applying origami and kirigami concepts to nanomembranes, designers leverage the fact that scaling down in thickness dramatically increases flexibility. An extremely thin membrane (on the order of 10–100 nm) can often be bent to a small radius without plastic deformation or fracture, because bending-induced strain scales with thickness[5,7] (**Figure 3a**). Ultra-thin films can thus accommodate sharp curvatures elastically. The favorable bending mechanics of nanomembranes are a key enabler for microscale origami and kirigami. For example, graphene monolayers (0.34 nm thick) and other 2D materials exhibit exceptional bendability[14,62] (Figure 3b). They can be scrolled or folded with a radius of curvature on the order of tens of nanometers without breaking. Even a semiconductor nanomembrane

(~100 nm thick) is vastly more pliable than a bulk wafer, allowing phenomena like the rolling or buckling of silicon that would be impossible in a thick substrate.[63] This is quantified by the Föppl–von Kármán (FvK) number, which compares a membrane's in-plane rigidity to its bending rigidity.[14] Atomically thin or ultrathin membranes have extremely high FvK numbers, meaning they prefer bending or crumpling out-of-plane rather than stretching in-plane. As a result, nanomembranes can undergo large out-of-plane deformations (folds, scrolls, wrinkles) with minimal in-plane strain. This is a favorable scenario for origami/kirigami, since it reduces the risk of material failure due to stretching.

Despite their flexibility, nanomembranes do have mechanical limits, and understanding stress distributions during folding is critical. When a membrane is folded along a line, the material at the fold experiences bending strain $\epsilon = t/2R$ (for thickness t and fold radius R). If R is too small or t too large, this strain can exceed the material's elastic limit, causing cracking or plastic deformation. One strategy to avoid this is to localize bending to the designed hinge regions. By making the membrane locally thinner or softer along intended crease lines, one can ensure that bending (and thus strain) concentrates there, while the adjacent panels remain essentially rigid. Simulations have shown that if the thickness of a crease region is less than about one-third the panel thickness, the thick panels will undergo negligible deformation and the thin creases will absorb the necessary strain[25] (Figure 3c). Increasing the crease width (spreading the curvature over a slightly wider zone) and decreasing its thickness both help to reduce the maximum strain in the material, thus preventing failure. In practical terms, this could be achieved by a two-step etching process that leaves half-etched lines on the membrane to act as creases. It is also possible to lithographically pattern the creases as winding springs, which has been implemented on materials with high modulus such as silicon nitride. This method also effectively reduced the bending stiffness of the crease and the bending strain in the material, therefore allowing repeatable folding up to tens of thousands of times without any breaking[32] (Figure 3d). Another method is to use a bilayer material: for example, a soft polymer strip on the back of a stiff metallic film can serve as a hinge that endures large bending while the metal remains elastic[64] (Figure 3e).

Kirigami offers an alternative means of managing strain: by removing material to create cuts or slits, one allows the membrane to deform out-of-plane without stretching the bulk of the material. A well-designed kirigami pattern can thus dramatically reduce in-plane strain concentration during a folding or buckling process. The earlier example of a cross-cut converting a square membrane into a pyramid is illustrative.[6] Finite element analysis showed that the cuts segment the membrane in such a way that each panel can bend and rotate with much lower internal strain, and the narrow connecting hinges between panels experience only moderate bending stress.[6] Essentially, the cuts play two critical roles: i) they eliminate large, continuous regions of the film that would otherwise develop damaging localized deformations (e.g., wrinkling or tearing under compression), and ii) they prevent self-intersection or jamming by providing clearance as different parts of the structure rotate and fold[65] (Figure 3f).

In summary, the key mechanical considerations for nanomembrane origami/kirigami are: keep bending strains below critical values (via thin hinges, large radii, or cuts), exploit the naturally low bending stiffness of thin films to enable folding, and minimize any required in-plane stretching. When these criteria are met, even rigid materials like silicon or silicon nitride can undergo dramatic shape changes elastically. Indeed, it has been observed that 2D materials such as graphene, WSe_2, and SnS_2 can be bent, twisted, and stretched to extreme degrees, thanks to their atomic-scale thickness and strong in-plane bonding[14,62,66] (Figure 3g). Such findings reinforce that, by harnessing proper design, nanomembranes can achieve mechanical transformations that bridge the gap between traditional rigid devices and the flexible, foldable systems sought in emerging technologies.

2.3. Microactuation Mechanisms

To realize the fold-up of a nanomembrane into its 3D form, an actuation mechanism is required. At the human scale, we simply use our fingers to fold paper; at the micro/nano-scale, a variety of stimuli can be employed to drive folding, including capillary forces, residual stress release, mechanical buckling, stimuli-responsive materials, magnetic/electric fields, and even direct-write techniques like focused ion beam (FIB) stress induction. The choice of actuation depends on the context: some devices are intended to self-assemble (fold automatically once released from a substrate), while others are meant to be dynamically reconfigured on demand. The major microactuation strategies are discussed below.

One elegant method to fold nanomembranes is using the surface tension of liquids. When a liquid droplet contacts a thin, flexible film, the liquid's surface tension can wrap the film around the droplet as it minimizes the surface energy, essentially performing origami without hands. This phenomenon, known as capillary origami, was first demonstrated with elastomer and polymer films, and later adapted to smaller, inorganic membranes. For example, Gracias and coworkers showed that a millimeter-scale hydrogel or thin metal/polymer bilayer can self-fold into a closed polyhedral container when a solvent droplet placed on it evaporates.[67] This concept is later adapted to the spontaneous folding of single-crystalline silicon sheets (1.25 μm thick).[68] Other than water droplets, melted solders can also be used to pull the panels together in a microscale origami.[67] Recent work demonstrates similar concepts based on oil droplets dissolving into the bulk solutions, folding a monolayer of MoS_2 into a micron-scale polyhedron[69] (**Figure 4a**). A key feature is that capillary origami typically results in a single, stable folded state once the liquid dries, which is useful for self-assembly (though not for reversible actuation). Moreover, since capillary forces act uniformly, they can fold multiple hinges simultaneously. Capillary folding is particularly attractive for parallel assembly: one can pattern many flat devices on a chip and then introduce a liquid to fold all of them together.

Another widely used mechanism is incorporating internal stresses that cause a flat membrane to spontaneously buckle or roll up when released from a substrate.[70] Researchers have used this effect to create self-rolling nanotubes and scrolls: a classic example is evaporating metal on strained polymers, which then roll up into tubes when freed.[11] In the context of origami, one can

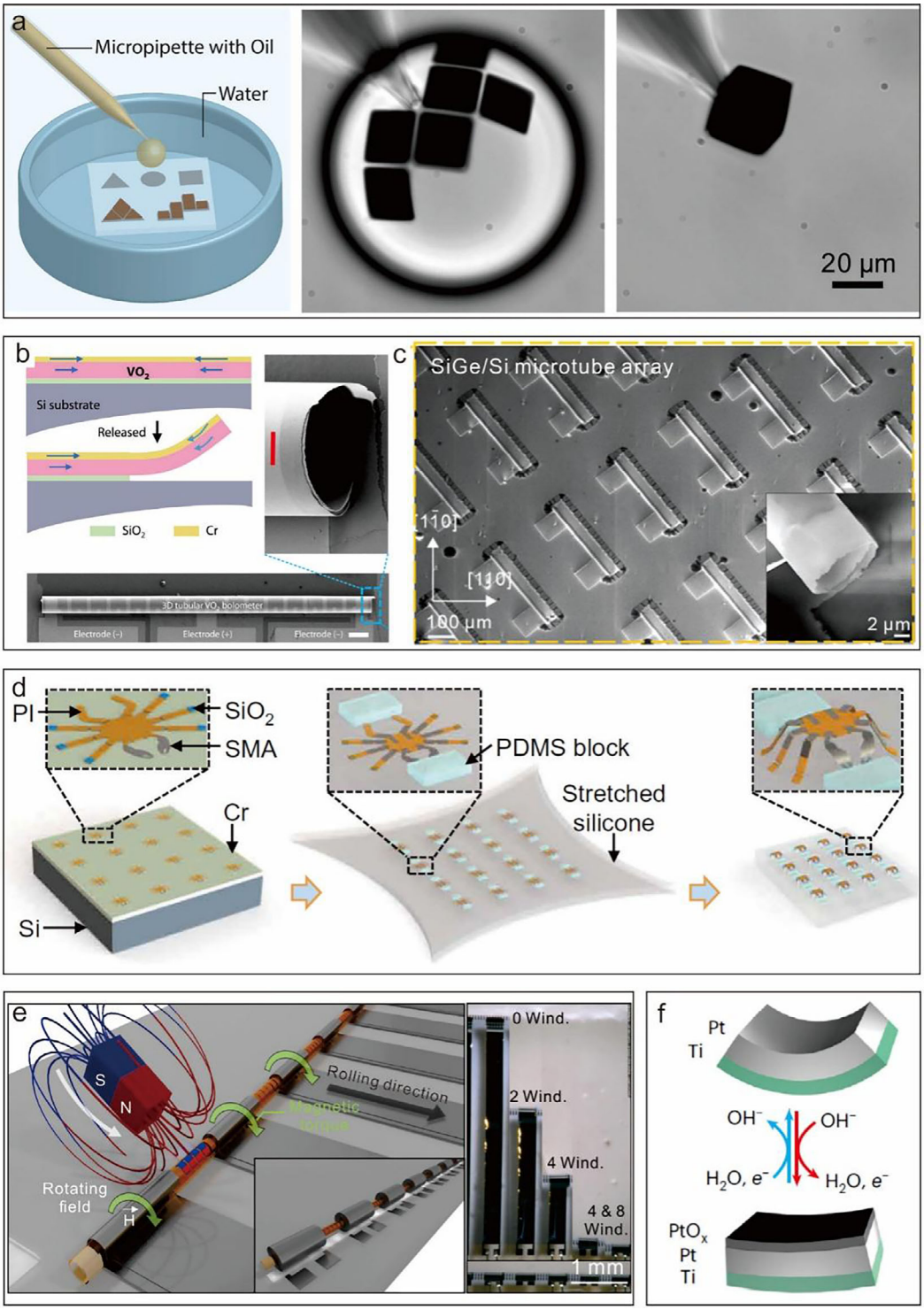

Figure 4. Microactuation mechanisms. a) The experimental setup and folding of shape nets (Cu panels and MoS_2 hinges) into a cube and a tetrahedron. Reproduced with permission.[69] Copyright 2019, ACS. b) Illustration of VO_2/Cr bilayers with compressive strain on silicon wafers before and after removal of SiO_2 sacrificial layer. Focused and side view of a single microtube. Scale bar, 50 μm. Reproduced with permission.[73] Copyright 2023, AAAS. c) SEM image of the Gr-readout SiGe/Si tubes. Inset: channel area of Gr-readout SiGe/Si microtube. Reproduced with permission.[74] Copyright 2025, Wiley. d) Schematic illustration of the fabrication process. Reproduced with permission.[78] Copyright 2022, AAAS. e) Assembly of capacitors in an external rotating magnetic field by winding the unstrained capacitor nanomembrane stack onto the magnetic rotor. (Inset) Assembled capacitors after fabrication. Time sequence of the winding process. The bottom image shows an assembled array of capacitors. Scale bar is 1 mm. Reproduced with permission.[12] Copyright 2019, Springer Nature. f) Redox reactions drive bending in an atomically thin SEA made of a platinum strip capped on one side by a titanium film. Reproduced with permission.[65] Copyright 2025, Springer Nature.

program patterns of strain such that specific regions bend in specific directions. Huang et al. developed SiN_x bilayers deposited by high-frequency and low-frequency plasma-enhanced chemical vapor deposition with carefully designed residual stress mismatch, resulting in self-rolled-up microtubes once released from the substrate for on-chip inductors[71] and transformers.[72] Similar stress mismatch also exists in many other bilayer material systems, such as VO_2/SiO_2[73] (Figure 4b), Si/Ge,[24] and SiGe/Si[74] (Figure 4c) due to different lattice constants and/or thermal expansion rates. Some material systems may have an intrinsic stress gradient, such as the nanocrystalline diamond nanomembranes deposited by chemical vapor deposition, as shown in the work by Tian et al.[75] Further, any method that creates a nonuniform stress distribution (e.g., thermal gradients, volume change in a responsive layer, etc.) can result in self-folding. A notable example is the use of a responsive bilayer: one layer expands or contracts in response to stimuli (heat, light, humidity), bending the composite. Recently, Jiafang Li and coworkers developed nano-kirigami transformation techniques on suspended 2D nanomembranes.[28,76] When irradiated with low-dose focused ion beam irradiation, tensile stress is induced, resulting in upward deformations in the kirigami structures. This technique is of particular interest to optical metamaterials.

Direct mechanical manipulation remains a straightforward way to induce folding, especially through controlled buckling. A powerful strategy introduced by Rogers and co-workers is to use a soft elastomer substrate to transform planar microstructures into 3D via buckling instabilities.[6,49] In this approach, a 2D patterned nanomembrane (e.g., a lattice of islands connected by narrow strips) is selectively bonded to a stretched elastomer. When the pre-strain in the elastomer is released, the differential contraction causes the bonded parts of the membrane to buckle out of plane, lifting the free parts into a predetermined 3D configuration. By designing the pattern of bonding sites and the geometry of the cuts/creases, one can achieve a rich variety of pop-up 3D shapes. This mechanically guided origami is fast (the transformation happens almost instantaneously upon release) and parallel (the whole wafer can buckle at once). It was used to create arrays of 3D microstructures in materials including silicon, metals, and 2D semiconductors, which have found numerous applications in flexible electronics.[77] Recent advancements have also led this technique to robotic applications, such as a microrobot crawling on various surfaces[78] (Figure 4d) and a microflier that can be widely dispersed for wireless sensing.[31] These works exemplify the wide applicability of this technique for the fabrication of 3D microstructures in various forms.

By integrating magnetic materials into selected regions of a nanomembrane, one can use external magnetic fields to induce folding motions. Cui et al. reported a micromachine embedded with nanomagnetic arrays, exhibiting reversible folding behavior under the control of external magnetic fields.[32] In a magnetic rolling origami by Gabler et al., high-aspect-ratio nanomembrane components were embedded with ferromagnetic elements[12] (Figure 4e). Electric stimuli have also been employed in conjunction with specialized materials. For example, the microscale metasheet robots developed by Liu et al. were fabricated flat with built-in hinges (gold/platinum bimorphs) that can be electrochemically actuated with electrical stimulus.[65] In this work, electrical signals allow effective control of independent regions in the same microrobot with phase delays, inducing effective locomotory gaits[65] (Figure 4f). The thermal bimorph effect (two-layer hinges that bend with temperature due to differential expansion) is another common mechanism in microscale origami that can drive folding.[13]

Each actuation method has its pros and cons. Capillary and residual stress methods are excellent for parallel self-assembly of 3D structures during fabrication. They are single-shot and require no tethers or wires, ideal for creating a 3D structure that will remain in place. However, they offer less control once the structure is formed (not easily reversible or tunable). Mechanical and stimuli-responsive actuation (including magnetic, electric, and thermal actuation), on the other hand, can be reversible and even continuous, enabling reconfigurable devices (e.g., a robot that folds and unfolds repeatedly, or a metamaterial that changes state under different stimuli). The trade-off is that these often need external input (magnetic fields, electrodes, lasers) and special stimuli-responsive materials. Another challenge is precision: achieving a desired final fold angle or alignment can be tricky, especially if multiple hinges must coordinate.

In summary, a rich toolbox of micro/nano actuation mechanisms now exists for origami and kirigami systems. From passive self-folding driven by capillarity or residual stress, to active shape-morphing using environmental stimuli or on-board actuators, these approaches enable the stunning transformations from flat films to intricate 3D microstructures. As actuation techniques improve in precision and integration, we can expect increasingly complex and functional 3D micro-architectures to emerge, moving the field closer to the vision of microsystems that can alter their form and function on demand.

3. Fabrication Methods

3.1. Patterning the Creases and Cuts

Realizing origami and kirigami designs on nanomembranes begins with high-precision patterning of the 2D membrane to define the locations of folds (creases) and cuts. The fabrication typically leverages planar microfabrication techniques adapted from the semiconductor industry, starting with a thin film material on a substrate. A common approach is to use photolithography or electron-beam lithography to pattern resist lines where cuts or grooves are needed, followed by etching of the nanomembrane. In the case of kirigami, through-thickness cuts are made to fully release certain edges or create apertures. In the case of origami-style creases, one can do a partial etch to thin the membrane along a line, or deposit a different material along the would-be crease to act as a hinge. For example, one might etch narrow trenches halfway through a silicon membrane to create "flexural hinges" that bend easily, while leaving the rest thick to be rigid panels[25] (**Figure 5a**). Alternatively, a focused ion beam can directly write crease lines by implanting Ga^+ ions, which locally plasticize or weaken the material, effectively creating a hinge that will preferentially bend there during folding.[79] FIB patterning has been used to realize some of the smallest origami structures, including nanoscale cubic boxes and mechanisms, by "drawing" the crease pattern on a suspended nanomembrane, which then folds upon release[27] (Figure 5b). However, FIB is slow

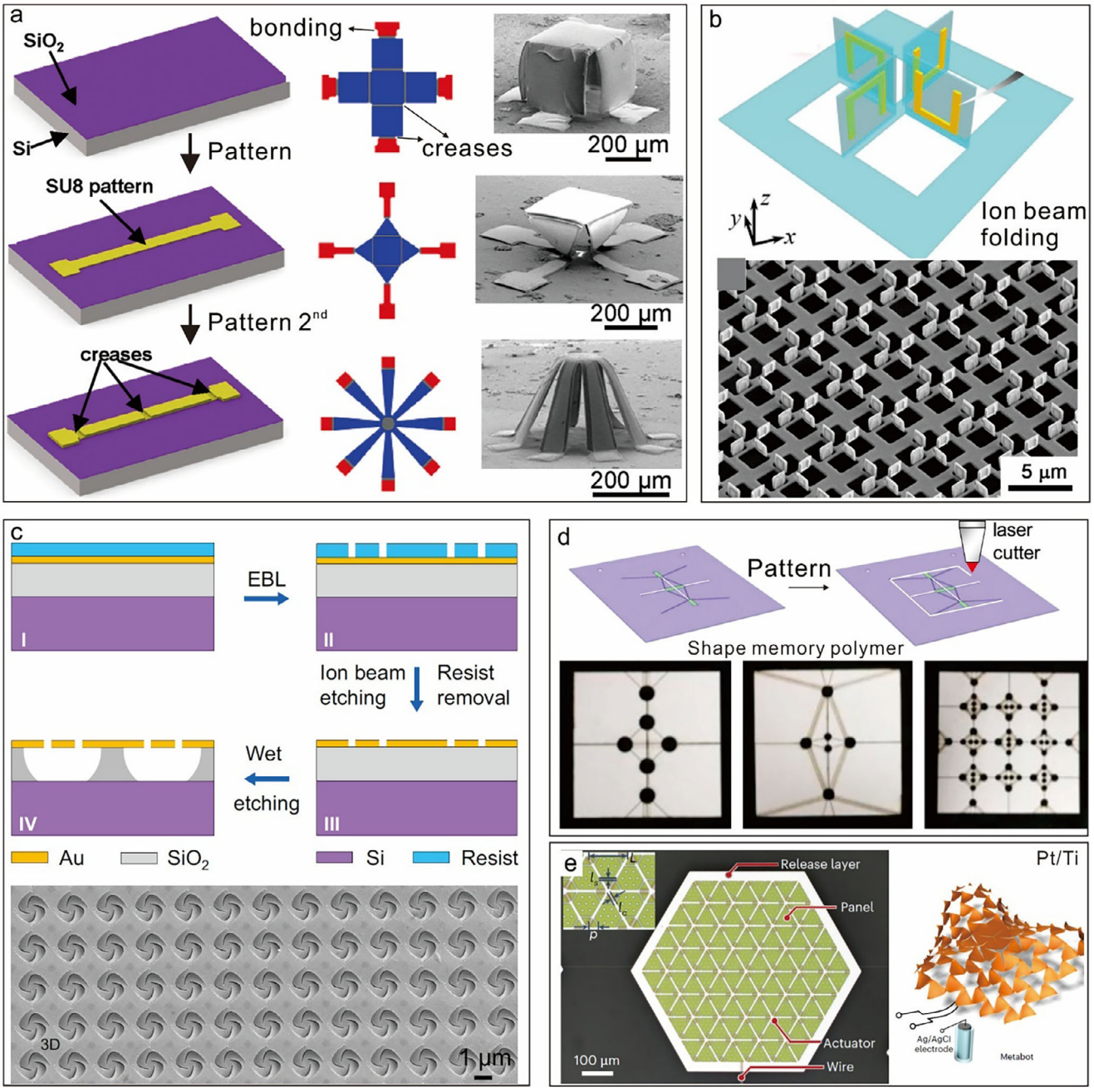

Figure 5. Patterning the creases and cuts. a) Schematic illustration of steps for fabricating 3D origami structures in polymer (SU8) and experimental and computational studies of various origami structures. Reproduced with permission.[25] Copyright 2016, Wiley. b) A toroidal molecule folded by ion beam and SEM images of toroidal metamaterial array in 52° tilted view. Reproduced with permission.[27] Copyright 2017, Wiley. c) Flow chart of the fabrication process on an Au/SiO_2/Si chip and top-view SEM images of deformed 3D pinwheels. Adapted with permission.[28] Copyright 2021, Springer Nature. d) Schematic of fabrication of an active kirigami metasheet and corresponding proof-of-concept experiments fabricated trilayer kirigami composite sheets. Reproduced with permission.[51] Copyright 2019, National Academy of Sciences. e) An optical microscopy image of a metabot with 96 panels and a metabot sheet capable of adopting a variety of shapes on the basis of which unit cells are electrically activated. Reproduced with permission.[65] Copyright 2025, Springer Nature.

for large areas, so lithographic patterning is preferred for batch fabrication.

For kirigami patterns involving complex cuts, etching (using reactive-ion etching or wet etchants) after optical lithography or e-beam lithography provides both precision and parallelism[28,76] (Figure 5c). One noteworthy example is the fabrication of a graphene kirigami spring: an e-beam defined a series of slits in a graphene sheet on a substrate, and after etching and release, the graphene could be stretched like a spring without breaking.[14] The minimum feature size (slit width, hinge width)

depends on the resolution of the lithography and the thickness of the membrane—thinner membranes can accommodate narrower hinges without snapping. One must also carefully design joining points in kirigami patterns. If the goal is a contiguous structure that folds up, the cuts should not completely sever the membrane into disjoint pieces. Carefully designed hinges based on the origami concept are implemented for microscale kirigami devices[51,65] in order to avoid such breaks (Figure 5d,e).

To summarize, the patterning step uses microfabrication techniques to turn a continuous thin-film material into a patterned membrane with the desired origami/kirigami design. Key techniques include lithographic etching for cuts and selective thinning, FIB milling for fine or post-fabrication patterning, and deposition of hinge materials. The outcome of this step is a flat, patterned nanomembrane (usually still adhered to its original substrate) that contains all the cuts, crease lines, and hinge features required for the 3D shape.

3.2. Detachment and Transfer

Once the membrane is patterned, the next crucial step is to detach it from the substrate so that it becomes free to move and fold. Nanomembranes are often fabricated on a substrate (like silicon or glass) for convenience and support during patterning. To deploy the origami/kirigami, the patterned membrane must be released. There are a few common approaches:

Surface micromachining with sacrificial layers is a classic method that borrows from Micro-Electro Mechanical Systems (MEMS) processing. The nanomembrane is deposited on top of a sacrificial layer (such as a polymer or oxide) that can be removed selectively. For example, in semiconductor processes, one might use a silicon-on-insulator (SOI) wafer where the top silicon layer (which becomes the nanomembrane) is separated from the bulk silicon by a buried oxide layer. After patterning the top silicon, an etchant (like HF) is used to dissolve the oxide, thus freeing the silicon nanomembrane[80] (**Figure 6a**). Similarly, metal or polymer films can be released by etching away an underlying buffer layer (e.g., dissolving a thin polymer underlayer[81]), as shown in Figure 5b. The freed 2D membrane can then be folded by the mechanisms discussed. This approach has been used in self-folding origami devices, such as microgrippers fabricated on a soluble polyvinyl alcohol (PVA) layer released in water[29,82] (Figure 6c). Also, many devices adopt aluminum as the sacrificial layer underneath,[65,83] which can be readily removed by an aluminum etchant compatible with microfabrication processes. One must take care that the release etch does not damage the thin structure. Very often, critical point drying or controlled drying techniques are used to avoid stiction (unwanted sticking of the membrane to the substrate due to capillary forces during drying). For this purpose, dry etching of the sacrificial layers by gas etchant receives increasing attention, such as using XeF_2 to etch away germanium[71] or silicon layers[30] (Figure 6d). In more complex assemblies, multiple sacrificial layers can allow stepwise release of different parts. Recent advancements demonstrate the release of nanomembranes without using any sacrificial layers, taking advantage of the intercalation of tiny droplet.[76,84] This method offers a simple and versatile approach for the release of origami and kirigami devices made by various materials on different substrates.

Pioneered by John Rogers' group, transfer printing techniques have become a staple for assembling 3D origami and kirigami microstructures[85] (Figure 6e). In this approach, the 2D pattern is first fabricated on a native wafer, but then picked up by an elastomeric stamp (like PDMS) and transferred to a target substrate. For origami/kirigami, one might fabricate the pattern on a silicon wafer with a surface treatment that allows it to peel off (for example, a low-adhesion surface or a UV-curable release layer). A PDMS stamp is pressed onto the wafer, and when retracted, it lifts the thin membrane pattern off, which can then be "printed" onto a target substrate. It is worth noting that this transfer process requires proper tuning of the adhesion forces at the interfaces. For a proper transfer, the adhesion between the stamp and the nanomembrane should be larger than that between the source substrate and the nanomembrane, but smaller than that between the target substrate and the nanomembrane.[85] This process has been further adapted to the transfer and release of microscopic origami robots.[30] A photoresist layer was spin-coated first on top of the robots, which adheres to the PDMS, allowing the robot to be peeled off together with the stamp. When placing the PDMS stamps into solutions and etching away the resists, the robots were then released and ready for further origami transformation.[30] These types of transfer printing techniques are mainly suitable for nanomembranes or devices in planar forms, since 3D microstructures may be crushed by the mechanical pressing using a stamp. To address this, Yan et al. developed a transfer technique for 3D microstructures using wax stamps[86] (Figure 6f). Melted wax can encapsulate the 3D microstructures for transfer printing, which can then be dissolved by toluene at 70 °C. With this technique, a 3D microstructure can be safely transfer printed without altering its geometry.

In summary, the detachment and transfer stage transitions the nanomembrane from the fabrication environment to the assembly environment. It leverages MEMS release techniques (sacrificial layers, etching) and innovative printing methods to preserve the integrity of delicate patterns. Successful release yields a freeform 2D sheet that's ready to be folded.

4. Device Applications

4.1. Optoelectronics Devices

Optoelectronic devices that source, detect, or manipulate light can greatly benefit from 3D structural formats. By moving from a flat device architecture to a folded or curved one, one can achieve wider fields of view, multi-angle functionality, improved light trapping, and tunable optical responses. Researchers have exploited origami and kirigami designs to create innovative optoelectronic systems such as flexible 3D displays, folded photodetector arrays, and tunable optical metasurfaces.

One of the early successes of micro-origami in optoelectronics was in creating stretchable and deformable displays. Rogers and colleagues pioneered a stretchable inorganic Light Emitting Diode (LED) matrix that could wrap around curved surfaces[87,88] (**Figure 7a**). The device wasn't explicitly described as origami, but it used mesh layouts (akin to kirigami cuts) to allow bending. Building on that, recent work has demonstrated fully 3D

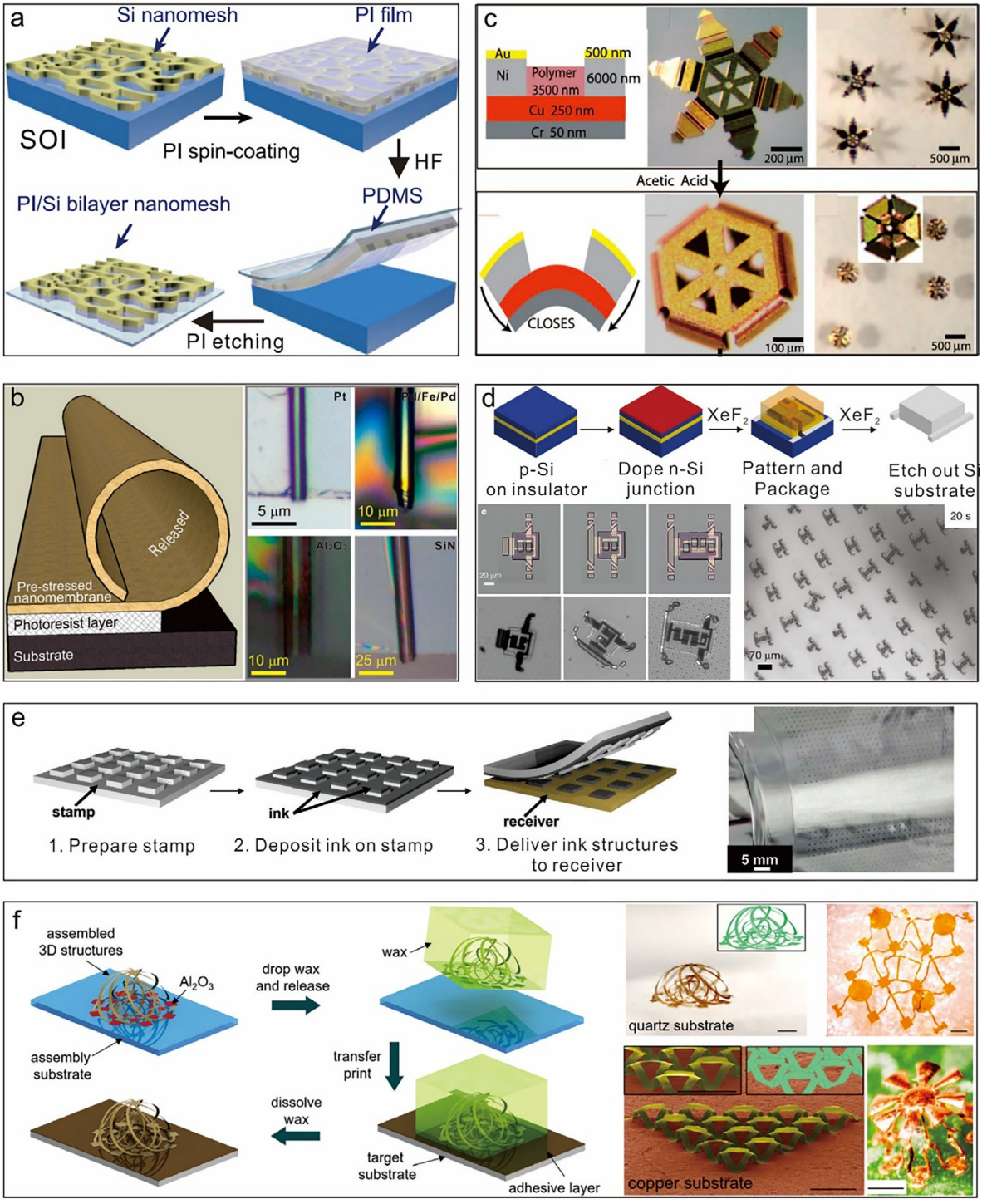

Figure 6. Detachment and transfer. a) Schematic illustration of the transfer process to achieve stretchable PI/Si bilayer nanomeshes. Reproduced with permission.[80] Copyright 2019, Springer Nature. b) Schematic diagram illustrating the roll-up process of a nanomembrane into a tube on photoresist; optical images of rolled-up nanomembranes made out of different materials. Adapted with permission.[81] Copyright 2008, Wiley. c) Schematic diagram of the trilayer hinge joint between two Au-coated Ni phalanges. Optical microscopy image of a microgripper in water. Reproduced with permission.[29] Copyright 2008, ACS. d) Schematic of the fabrication process (Methods) and optical images of robot designs before and after release. Reproduced with permission.[30] Copyright 2020, Springer Nature. e) Additive transfer exploits a stamp that is "inked" with a material of interest, using processes such as physical vapor deposition, solution casting/assembly, or physical transfer. Large-scale collection of structures (~1600 in a square array with pitch of 1.4 mm) printed onto a thin, flexible sheet of plastic. Reproduced with permission.[85] Copyright 2012, Springer Nature. f) Schematic illustration of the method for a representative case of a multilayer, nested cage structure and optical micrographs, SEM images, and FEA results (insets on the right top) of a trilayer nested cage of silicon on a different substrate. Scale bar, 500 μm. Reproduced with permission.[86] Copyright 2017, National Academy of Sciences.

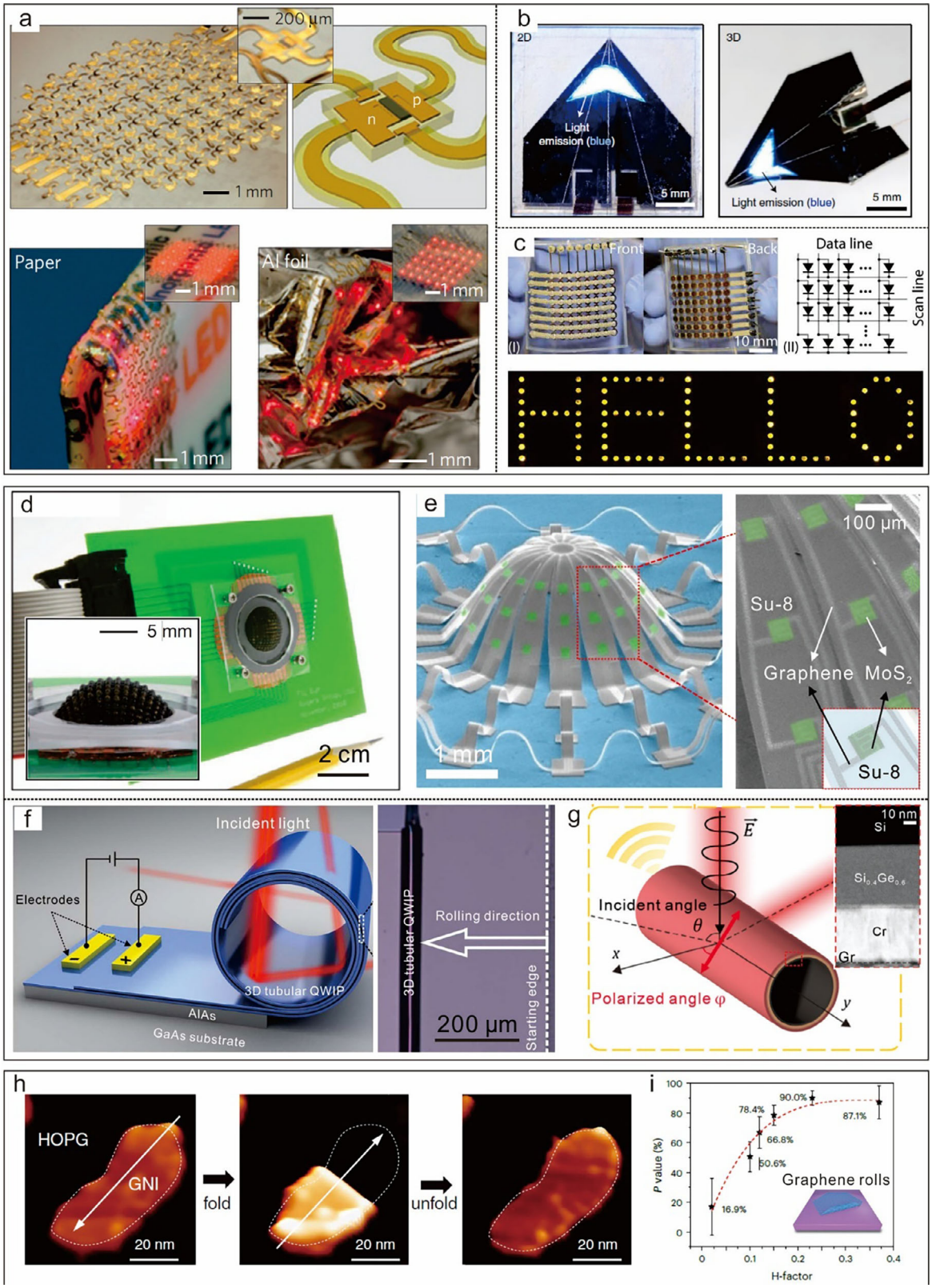

foldable displays using mechanical assembly. Kim et al. produce Quantum Dot Light Emitting Diode (QLED) that reversibly transform into complex three-dimensional architectures with an ultra-small bending radius of 0.047 mm, culminating in a foldable passive-matrix array capable of alphanumeric display and offering a scalable pathway to next-generation deformable display technologies[89] (Figure 7b). Hu et al. realize a mechanically robust, full-color flexible display that surpasses conventional color-filter gamuts, conforms to curved or epidermal substrates, and functions as a visible-light transmitter.[90] Su et al. introduced a multimodal 3D-printing strategy that suppresses film non-uniformity and mechanically reconfigures viscoelastic cathode droplets to enlarge polymer–metal junctions, culminating in the first fully 3D-printed, flexible 8 × 8 Organic Light-Emitting Diode (OLED) display with every pixel operating successfully[91] (Figure 7c). In these works, the LEDs are interconnected with flexible hinges, so that the whole assembly can deform. The implications are significant for wearable and curved displays, where conformability and durability are of great importance.

On the sensing side, folding light sensors into 3D configurations allows capturing richer information. A striking example is the "fly's eye" imaging system that uses a domed array of photodetectors to capture wide-angle images without aberrations, inspired by insect compound eyes[26] (Figure 7d). Ko et al. built such a device by electrically connecting tiny photodiode pixels on a stretchable membrane and then inflating it into a hemispherical shape according to origami-like deployment.[26] More directly, a 3D origami photodetector system was demonstrated in which photodiodes on different facets could measure the incident light's direction. Lee et al. demonstrated arrays of 2D material photodetectors integrated on a prestrained nanomembrane that, when released, buckled into hemispherical and prismatic shapes[92] (Figure 7e). These 3D photodetector architectures can detect not only light intensity but also the angle of incidence, since different facets of the curved array receive light from different directions.[92] Such functionality is highly desirable for artificial vision systems and motion tracking. Thus, origami/kirigami approaches can significantly improve optoelectronic device efficiency and coverage by utilizing 3D folded shapes.

Microtubular structures based on self-rolled-up techniques also demonstrate enhanced optoelectronic properties due to their unique advantages in light confinement.[7,93,94] For example, Wang et al. used a residual-stress-driven self-folding to create tubular quantum well infrared photodetectors (QWIPs)[95] (Figure 7f). These were essentially flat photodetector arrays that rolled up into cylindrical 3D cavities, enhancing absorption via multiple passes of light. The tubular QWIPs showed broadband enhanced responsivity and could detect infrared light from a ±70° field of view (nearly hemispherical coverage), far exceeding a flat detector's view. The 3D geometry was key to this performance-light entering the tube would strike the detector multiple times. Recently, by self-rolling VO_2 nanomembranes into a freestanding tubular geometry, Wu et al. delivered a one-step-fabricated bolometer that simultaneously boosts thermal insulation, broadband infrared absorbance, and temperature sensitivity.[73] Zhang et al. integrated a graphene readout layer with a silicon-based microtube architecture, realizing an omnidirectional photodetector that traps incident light, enhances polarization sensitivity, and achieves an ultrafast 75 ns response with an exceptional responsivity[74] (Figure 7g). Employed as a visible-light-communication receiver, the device attains 778 Mb s^{-1} over a 140° field of view while enabling polarization-encrypted links, holding promises towards high-performance, secure Internet-of-Things (IoT) optical networks.[74]

2D materials in 3D configurations also open optoelectronic possibilities. In Li et al.'s seminal work, a periodic wrinkle pattern in a MoS_2 monolayer is created, which generated an array of quantum dot-like regions with altered bandgap, thus forming a new optoelectronic crystal lattice.[96] This strain-induced patterning led to emergent photoluminescence properties not found in flat MoS_2, showcasing how out-of-plane deformation of a nanomembrane can tailor its optoelectronic behavior.[96] Similarly, folding graphene can open a bandgap or create localized states; researchers have used Atomic Force Microscopy (AFM) tips to fold graphene into nano-origami shapes that exhibit engineered electronic properties at the folds[97] (Figure 7h). A universal wax-assisted immersion strategy has been recently developed to roll graphene into left- or right-handed tubes, demonstrating tunable optical activities and chiro-electronic properties.[62] The resulting chiral rolls display room-temperature chirality-induced spin selectivity with >90 % spin polarization, and provide a scalable platform for advanced optoelectronic and spintronic technologies[62] (Figure 7i).

In summary, origami and kirigami bring substantial benefits to optoelectronics by enabling 3D device layouts and geometry-induced material properties. The ability to wrap sensors around a sphere, funnel light into curved surfaces, or dynamically tune optoelectronic properties by folding gives designers new degrees

Figure 7. Optoelectronics devices. a) Optical image of a 6×6 array of μ-Inorganic Light-Emitting Diodes (ILEDs) (100 μm × 100 μm, and 2.5 μm thick, in an interconnected array with a pitch of ~830 μm) with non-coplanar serpentine bridges on a thin (~400 μm) PDMS substrate (left-hand frame). Optical image of an array of μ-ILEDs (8 × 8) on a piece of paper and Al foil. Reproduced with permission.[87] Copyright 2010, Springer Nature. b) Photographs of the fabricated QLEDs using the airplane pattern. Reproduced with permission.[89] Copyright 2021, Springer Nature. c) Images of a completed OLED display, the light emission of which was viewed from the backside, and a schematic circuit and driving mechanism of the OLED display. Image of the word "HELLO" while the text scrolled on the 8 × 8 OLED display. Reproduced with permission.[91] Copyright 2022, AAAS. d) Photograph of a completed camera mounted on a printed circuit board as an interface to external control electronics, and an Image of a representative system after hemispherical deformation. Adapted with permission.[26] Copyright 2013, Springer Nature. e) Colorized SEM image of MoS_2 photodetectors consisting of MoS_2 (green), graphene (light gray), and SU-8 (gray) on the hemisphere with 3D interconnects. Magnified view of the SEM image in (b) and corresponding FEA results for the strain distribution. Adapted with permission.[92] Copyright 2018, Springer Nature. f) Schematic diagram of a 3D tubular QWIP device and Optical image of a complete 3D tubular QWIP. Adapted with permission.[95] Copyright 2016, AAAS. g) Schematic diagram of Gr-readout SiGe/Si microtube photodetector and TEM image of rolled-up Gr/SiGe/Si microtube. Adapted with permission.[74] Copyright 2025, Wiley. h) The series of STM images shows a sequence of the folding and unfolding of a GNI along the direction indicated by the white arrows. HOPG, highly ordered pyrolytic graphite. Reproduced with permission.[97] Copyright 2019, AAAS. i) Dependence of the spin polarization, P, on the H-factor of the rolls. Reproduced with permission.[62] Copyright 2025, Springer Nature.

of freedom. As fabrication and integration improve, one can envision high-resolution foldable camera sensors (providing eagle-eye vision in a compact package), shape-shifting optical communications devices (that adjust their beam profiles), and even origami-inspired light modulators for VR/AR displays that conform to curved form factors. The convergence of 2D materials with origami techniques appears particularly fruitful, since many 2D materials are optoelectronically active and benefit from the strain and geometry control that folding affords.

4.2. Transformable Microrobots

One of the most exciting frontiers for origami/kirigami nanomembranes is in the creation of microrobots-tiny robots on the scale of millimeters or smaller—that can change shape and perform tasks in confined or dynamic environments. Traditional MEMS devices are mostly planar and have limited degrees of freedom, but by applying origami design, researchers are building microrobots that fold themselves into different 3D configurations to achieve complex motions like crawling, gripping, or swimming. These transformable microrobots take inspiration from origami, not just in structure but also in function: a single design can be reconfigured to execute multiple actions.

A pioneering example is the self-folding microgrippers for minimally invasive surgery.[98] Gracias and colleagues developed star-shaped polymer/metal bilayer devices (a few hundred μm across) that, when exposed to a stimulus (such as warmth at body temperature[99] or a chemical signal),[29] fold their "fingers" into a closed fist. These microgrippers begin as flat star-like patterns with hinged joints between each finger. Upon trigger, the hinges bend (e.g., through swelling or thermal expansion mismatch), causing the fingers to curl inward and grasp single cells[100] or a tissue[101] (**Figure 8a**). After performing the biopsy[82,102] or delivering a drug,[102] the grippers can even dissolve[103] (if made of bioresorbable materials) or be retrieved magnetically. This concept shows how origami-based designs yield practical microrobots that can autonomously change shape to interact with their environment, in this case, grabbing cells or biological samples. As fabrication techniques advanced, researchers took advantage of the 3D direct laser writing technique and fabricated microgrippers with programmable elasticity and magnetization profiles.[104] Consequently, these microgrippers are not only good at grasping and propelling single cells, but also capable of detecting forces as small as 0.5 pN[104] (Figure 8b). This work represents a versatile platform for bio-compatible microrobotics and precision single-cell manipulation.

Beyond grippers, significant progress has been made in developing origami- and kirigami-inspired swimming or crawling microrobots that use folding as a mode of movement. These advancements have been driven by the integration of flexible mechanical designs with actuation mechanisms (such as magnetic and electrochemical actuation), which enable precise control at microscopic scales. Early work demonstrated the ability to create helical-shaped microswimmers, which could swim in liquid environments using controlled magnetic fields.[105] This foundational concept of using external stimuli for propulsion paved the way for more sophisticated micromachines capable of shape morphing and complex reconfigurations. Cui et al. utilized single-domain nanomagnets to encode shape-morphing instructions into micromachines, enabling them to switch between various deformations[32] (Figure 8c). This approach allowed for precise control over the microrobots' transformations, making them capable of performing complex behaviors like "flapping" and "hovering".[32] In Figure 8d-i Miskin et al. demonstrated microrobots that are integrated with circuits including silicon p–n junctions and metal interconnect that can respond to low-voltage electronic control signals for precise motion control.[30] This work demonstrated the use of surface electrochemical actuators, which can be fabricated by standard semiconductor processing, so that the microrobots can be mass-manufactured at low cost. Based on similar actuators, Figure 8d-ii, Wang et al. further built electrically actuated artificial cilia to manipulate fluid flows with high precision at the microscale.[83] This research highlights the potential of cilia-inspired designs for microfluidic control and microrobotic applications, where localized actuation can enable complex tasks such as fluid pumping and manipulation. Further, Liu et al. introduced a new class of microscale robots with kirigami-inspired structures that enable rapid, complex shape deformations through independently actuated regions.[65] These robots can achieve sophisticated reconfigurations, making them highly versatile for applications requiring adaptive and multifunctional behavior. Smart et al. developed a new platform for microscopic robots capable of manipulating light using diffractive optics, offering new opportunities for imaging at the diffraction limit.[106] By combining nanomagnets with flexible mechanical elements, these robots have expanded the scope of their applications, particularly in fields like high-resolution imaging and force sensing,[106] beyond traditional biomedical engineering (Figure 8e).

Another exciting area is origami and kirigami-inspired microfliers that have shown significant advancement. Early studies, such as the work by Kim et al., utilized wind-dispersed seed designs, specifically those inspired by the Tristellateia species, to create 3D microfliers[31] (Figure 8f). These designs employed precise geometric transformations, where 2D precursors were mechanically buckled into their desired 3D configurations using controlled release techniques, enabling passive flight across large distances without power sources. This breakthrough highlighted the potential of using natural dispersal mechanisms in microfliers for environmental monitoring and other applications requiring wide-area coverage. Further progress was made in fabricating light-driven microfliers inspired by dandelion seeds. In a study by Chen et al., an ultralight, bimorph soft actuator was used to create a dandelion-inspired microflier capable of light-driven mid-air flight.[108] The design included a tubular actuator structure with a "pappus", which opened in response to light, altering its aerodynamic properties and allowing for controlled falling velocities.[107] This approach, which leveraged external light sources to control the microflier's motion, provided significant improvements in flight time and controllability compared to earlier designs. Building on these innovations, Yoon et al. introduced biodegradable 3D colorimetric microfliers that could monitor environmental parameters such as pH and heavy metals, offering a sustainable and effective solution for environmental monitoring in hard-to-reach areas.[108] Additionally, the work by Yang et al. further explored the

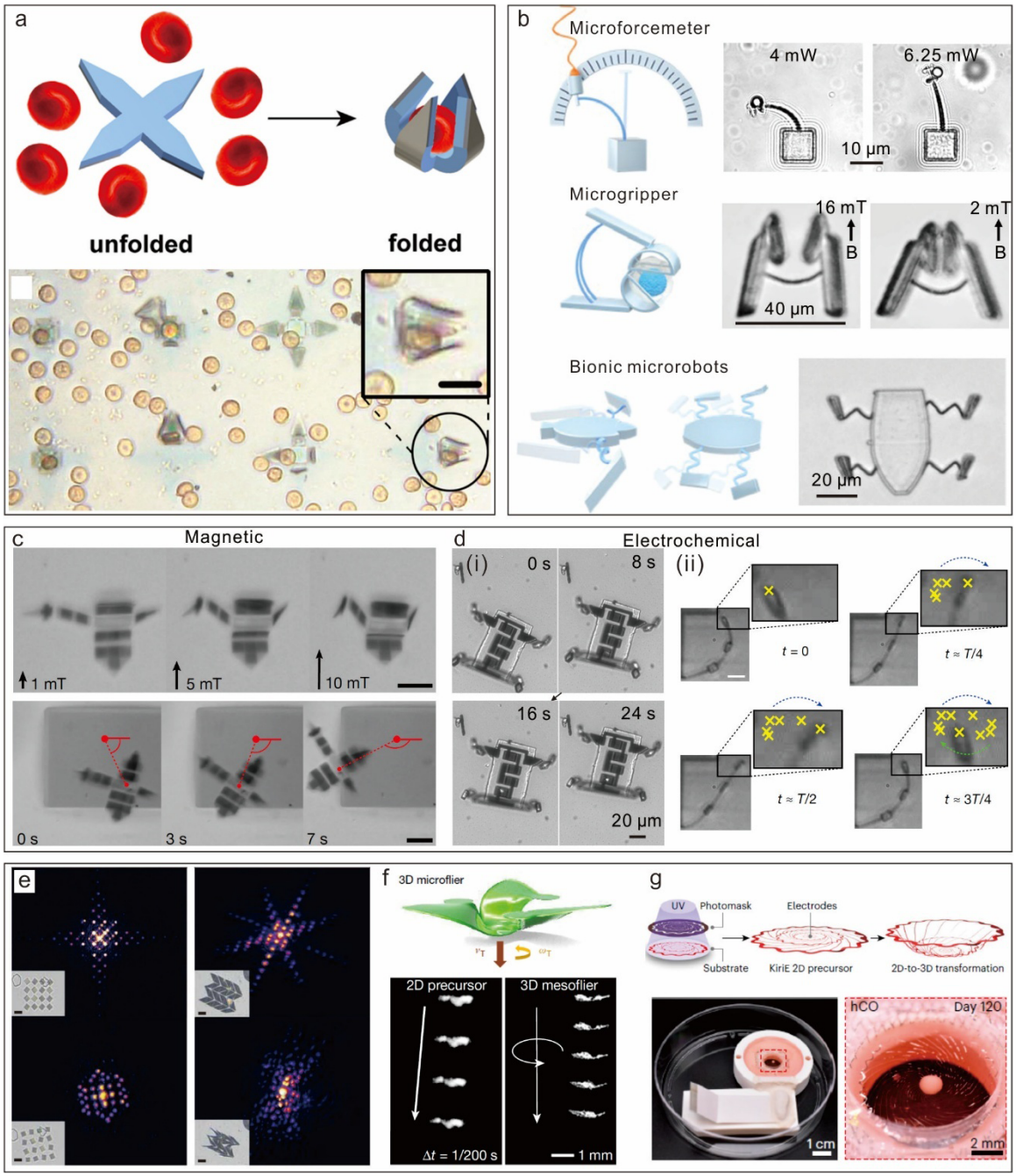

Figure 8. Transformable microrobots. a) Illustration of untethered single cell grippers and red blood cell capture, and red blood cells captured by the grippers. Scale bars are 10 μm. Adapted with permission.[100] Copyright 2014, ACS. b) Picosprings perform specific functions in customized soft micromachines with different configurations and corresponding experimental results. Adapted with permission.[104] Copyright 2024, Springer Nature. c) The optical microscope images of the microscale "bird" actuation by alternating magnetic field. Scale bars are 30 μm. Reproduced with permission.[32] Copyright 2019, Springer Nature. d) i) Montage of a real robot walking across a surface. Each frame is about 8 s apart. Reproduced with permission.[30] Copyright 2020, Springer Nature. ii) Non-reciprocal motion of one 50-μm-long cilium driven at 40 Hz. Magnified trajectories of the tip are shown at the top right. T is the period of the actuation cycle. The yellow cross symbols indicate the positions of the cilium tip at times $t = 0$, $t = T/4$, $t = T/2$, and $t = 3T/4$, corresponding to different moments in the stroke cycle. Scale bars are 50 μm. Reproduced with permission.[83] Copyright 2022, Springer Nature. e) Final magnetic dipole orientations. Diffraction images and (insets) real-space images of the metamaterial at 0 and 6 mT. Scale bars are 20 μm. Reproduced with permission.[106] Copyright 2024, AAAS. f) Schematic diagram of a rotating 3D flier and optical images of the 2D structure and the 3D mesoflier at various times during free fall. Reproduced with permission.[31] Copyright 2021, Springer Nature. g) The concept of vertically deformable kirigami electronics (KiriE) and the photographs show a spiral KiriE-hCO assembly. The zoomed-in photograph shows a spherical hCO on a spiral KiriE at day 120 of differentiation. Reproduced with permission.[111] Copyright 2024, Springer Nature.

application of light-responsive materials in creating robust and programmable microfliers, emphasizing the potential for adaptive control through programmable shape-deformation.[109] These developments demonstrate a trend towards increasingly sophisticated, energy-efficient, and adaptable microflier designs, driven by bioinspired structures. The integration of light-responsive materials and precise aerodynamic design is transforming the landscape of untethered, autonomous microfliers, opening up possibilities for a range of applications, from environmental sensing to advanced communications.

Beyond microfliers, origami/kirigami neural interfaces are rapidly maturing to address three persistent constraints: mechanical mismatch, minimally invasive access, and true 3D coverage. Early kirigami-inspired intracortical probes introduced slit patterns into polyimide backbones to drop the effective modulus from Gigapascal to Kilopascal levels, accommodate brain micromotion, and retain implantability, foreshadowing stretchable, conformal recordings.[110] Building on this foundation, "kirigami electronics" form basket-like 3D meshes that integrate with human cortical organoids in suspension and enable chronic electrophysiology for up to 120 days while preserving morphology, with compatibility for optogenetic and pharmacological modulation[111] (Figure 8g). In parallel, origami-inspired soft-fluidic actuation allows large-area electrocorticography grids to be folded for implantation and then expanded in situ to achieve centimetre-scale cortical coverage, validated in vitro and in porcine models.[112] Recent foldable thin-film opto-electro arrays further combine μ-LED neuromodulation with penetrating microelectrodes; an origami "bridge + trench" hinge converts a 2D precursor into a 3D array while providing insertion support and reducing fabrication complexity.[113] Finally, scalable 3D kirigami microelectrode arrays now deliver up to 512 electrodes across 128 shanks via matched-die forming and thermoforming, enabling in-vitro and in-vivo recordings with improved tissue integration and dense spatial sampling.[114]

In summary, the integration of origami and kirigami principles into microrobot design is evolving rapidly, with significant strides in fabrication techniques, actuation methods, and reconfigurable structures. These innovations are not only enhancing the functionality of microrobots but are also laying the foundation for future autonomous systems capable of performing complex tasks at the microscopic scale.

4.3. Reconfigurable Metamaterials

Metamaterials are engineered structures designed to achieve properties not found in natural materials, often through the arrangement of repeating unit cells rather than the composition of the base material. Origami and kirigami offer a powerful route to reconfigurable metamaterials-materials whose properties can be tuned or switched by folding transformations. In mechanical metamaterials, for instance, an origami pattern can endow a material with a tunable Poisson's ratio, stiffness, or shock absorption characteristics that change with fold angles. In electromagnetic metamaterials, folding can alter the relative positioning of resonant elements (split-ring resonators, dipoles, etc.), thereby shifting frequencies or polarization responses.

Early work in 2015 established the mechanical versatility of microscale origami units themselves. Silverberg et al. showed that a micro-origami device in square-twist forms becomes mechanically bistable once hidden facet-bending modes are engaged, yielding a switchable unit cell for architected lattices[13] (**Figure 9a**). In the same year, Blees et al. translated kirigami concepts to monolayer graphene, demonstrating >240% stretchability via cut rotation and flip while retaining electrical function.[14] Building on these insights, Lin et al. miniaturized Miura–Ori "zipper" tubes with two-photon lithography to realize the first fully 3-D microscale origami metamaterial; the lattice presents programmable stiffness anisotropy, reversible auxeticity (sign-switching Poisson's ratio), and multistability, recovering >90% strain after compression[115] (Figure 9b). Subsequent studies embedded active actuation and locking. Tian et al. introduced a Gaussian-preserved folding strategy in VO_2/Cr bilayers that delivers microsecond snap-through and non-volatile shape locking, allowing metamaterials to hold discrete mechanical states without continuous stimulus[116] (Figure 9c). Zhang et al. coupled kirigami microframes with liquid-crystal-elastomer "artificial muscles", achieving fully reversible, wireless thermal actuation and >50% in-plane reconfiguration in precisely printed micro-metastructures.[117] Most recently, Shi et al. exploited an I-shaped cutting motif in graphene to realize bidirectional stretchability (yield and fracture strains enhanced six- and ten-fold) and tunable negative Poisson's ratios, illustrating how geometric hierarchies can tailor the stress–strain envelope at the atomically thin limit.[118] These studies highlight a clear trajectory from passive bistable cells to actively reconfigurable, highly stretchable, and auxetic microscale origami/kirigami mechanical metamaterials.

Extending from mechanical to photonic regimes, kirigami/origami architectures also enable dynamic tunability in electromagnetic metasurfaces. For phase control, in-plane rotation of anisotropic scatterers imparts a geometric (Pancharatnam-Berry) phase, while out-of-plane displacement modifies the optical path to tune the propagation phase.[119,120] For amplitude, MEMS-actuated nano-kirigami can reversibly enhance or suppress reflectance/diffraction orders to yield high-contrast intensity modulation.[28] For polarization, 3D chiral deformations break mirror symmetry and induce circular dichroism and birefringence, enabling handedness-selective conversion and polarization-multiplexed functions.[22,121] Compared with phase-change materials and liquid-crystal/elastomer platforms, folding provides a geometry-driven route that is intrinsically broadband and low-loss on the photonic side, while trading off actuation speed and packaging/integration complexity. With these mechanism-level distinctions clarified, we next survey representative implementations to illustrate how folding is exploited in practice.

One of the early explorations in this field is Tao et al.'s work terahertz array in 2009, where split-ring resonators (SRRs) were lithographically attached to thermo-bimetal cantilevers; heating bent the SRRs out of plane, switching their magnetic and electric channels, and proving that mechanical folding could reconfigure a bulk electro-magnetic (EM) response in real time[122] (Figure 9d). Nearly a decade later, Liu et al. introduced one-step "nano-kirigami" on suspended gold films: ion-beam cuts and stress-guided buckling twisted each unit into a pin-wheel, amplifying intrinsic optical chirality by two orders

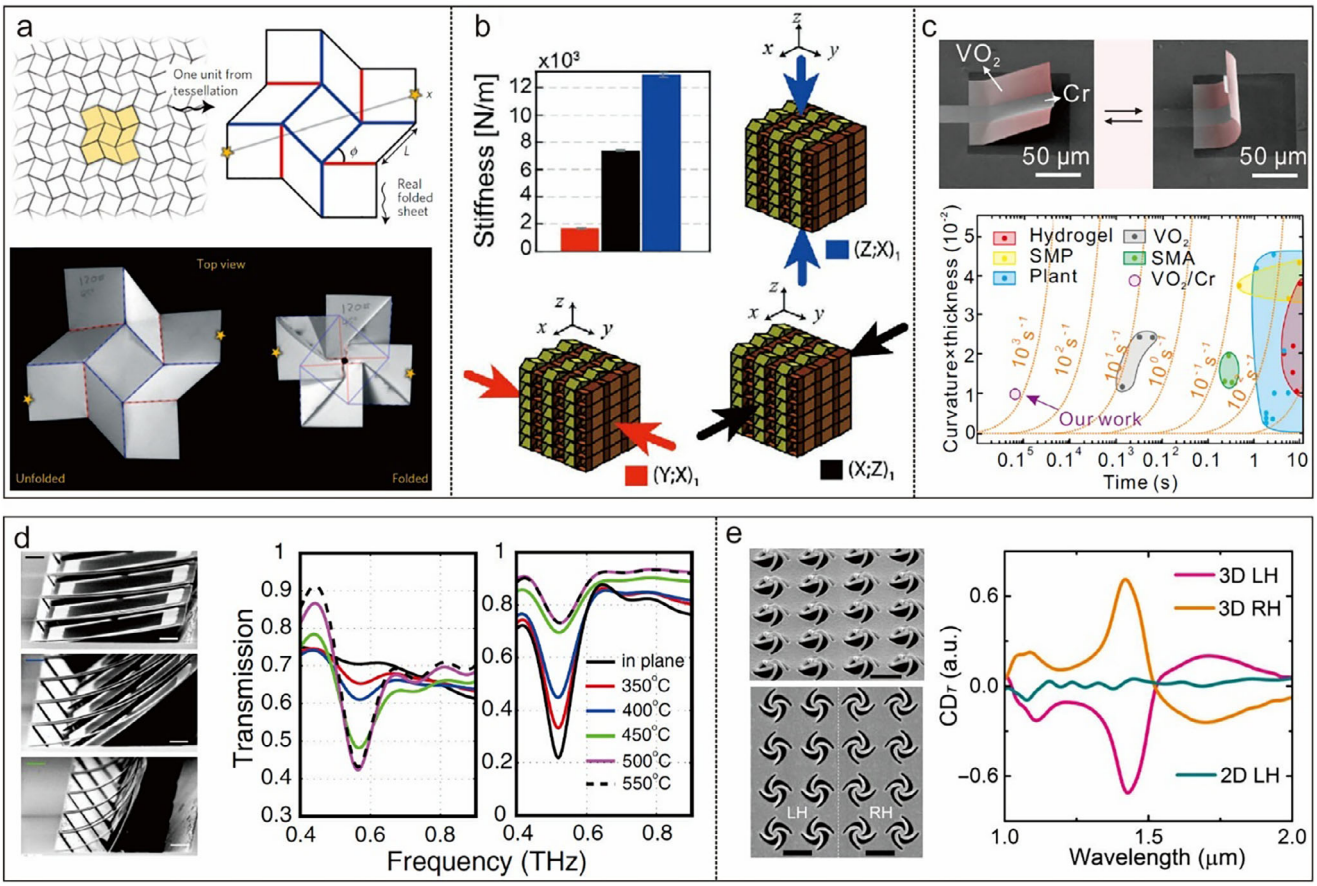

Figure 9. Reconfigurable metamaterials. a) The square-twist folding pattern is shown with the edges in black, mountain creases in red, and valley creases in blue. Photographs of a square twist with $\phi = 45°$ illustrate out-of-plane deformations, and the stars define x when the square twist is unfolded and folded. Reproduced with permission.[13] Copyright 2015, Springer Nature. b) Initial axial stiffness of the fabricated Configuration A metamaterial along Cartesian directions. Reproduced with permission.[115] Copyright 2020, Wiley. c) Anti-symmetric bending and actuation speed, orange dashed line, and relative curvature change of membrane-based actuators in the literature. Adapted with permission.[116] Copyright 2021, Springer Nature. d) SEM pictures showing the bending of the SRRs following KOH release (first picture) and rapid thermal annealing (RTA) at 400 and 450 °C. Magnetic Response (left) and electric Response (right): Transmission as a function of frequency for various orientations of the SRRs. Scale bars are 50 μm. Adapted with permission.[122] Copyright 2009, American Physical Society. e) SEM images of 3D pinwheel array and left-handed (LH) and right-handed (RH) 3D pinwheel arrays. Scale bars, 1 μm. Measured CD in transmission versus wavelength for 2D LH, 3D LH, and 3D RH pinwheels, respectively. Adapted with permission.[22] Copyright 2018, AAAS.

of magnitude and establishing nanoscale 3-D shaping as a route to strong circular-polarization selectivity[22] (Figure 9e). Building on similar concepts, Liu et al. reported a metasurface kirigami-raised blades whose controllable height tuned Fano resonances; the result was record-high, reversible circular dichroism per thickness under simple mechanical compression.[121] Chen et al. then integrated the architecture with reconfigurability: electrostatic attraction folded sub-micron pinwheels, delivering pixel-level phase modulation across the visible-NIR spectrum.[28] Most recently, Hong et al. freed nano-kirigami propellers from the substrate and steered them with optoelectronic tweezers; their 10 μm rotors act as reconfigurable, mobile meta-elements.[76] Liang et al. demonstrated a Complementary Metal Oxide Semiconductor (CMOS)-compatible silicon nano-kirigami platform on SOI with programmable plastic, fast-recovering elastic, and hysteretic modes; it enables repeatable electromechanical optical modulation and dynamic optical-information encryption, and the dielectric silicon base reduces Ohmic-loss limits relative to plasmonic metals.[123] Collectively, these milestones, including both substrate-integrated and fully untethered nano-kirigami represent adaptive electromagnetic metamaterials with tunable polarization, phase, and amplitude degrees of freedom. Such controllability is critical for applications like tunable filters, modulators, or beam steering devices in photonics.

In conclusion, origami and kirigami approaches are propelling metamaterials into a new realm of dynamic, reconfigurable performance. The ability to sculpt and rearrange matter at the microscale via folding is leading to materials whose properties can be programmed post-fabrication. This may lead to devices that are not only multifunctional but also intelligent—potentially forming the basis of active metamaterials that sense stimuli and reconfigure autonomously, like a smart skin that can change its stiffness, optical reflectance, or acoustic damping in response to the environment. Origami/kirigami provides the design and fabrication toolkit to build these future materials.

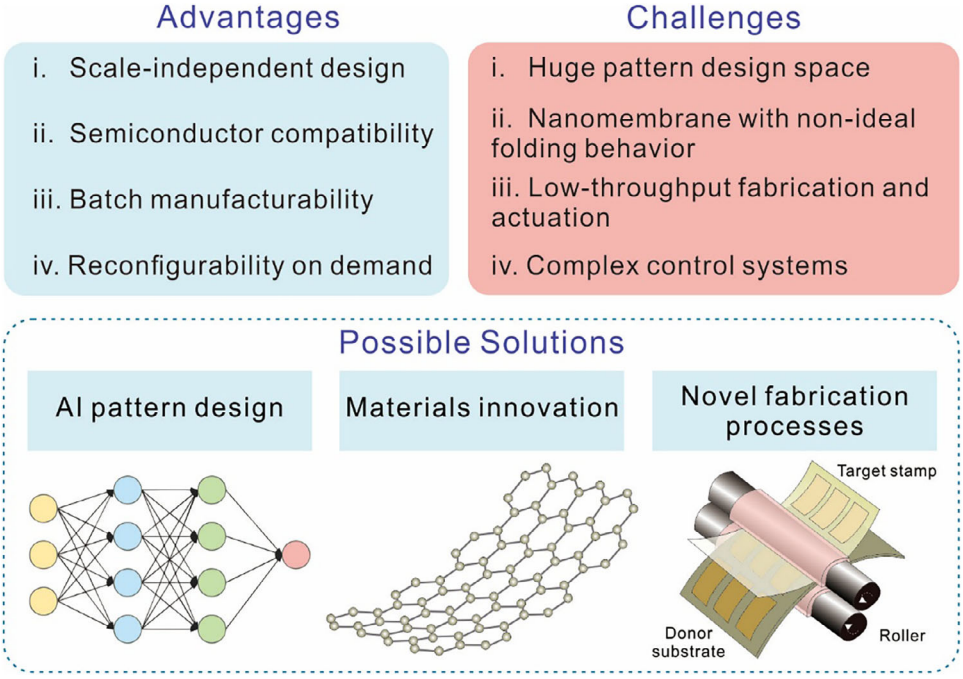

Figure 10. Advantages, challenges, and possible solutions for the future development of origami and kirigami on nanomembranes.

5. Conclusions and Perspectives

Origami and kirigami on nanomembranes have evolved from an intriguing idea to a versatile platform for building 3D micro/nanosystems. This review has outlined how ancient paper-folding art is translated into modern engineering: from design theory through fabrication to a broad range of applications. We first highlight how atomic-to-micron-thick films unlock extreme bendability while preserving the mechanical and functional integrity of advanced materials such as single-crystal Si, 2D semiconductors, and functional polymers. The core design rules are discussed, including the design of the crease and cut patterns that translate to tunable mechanical properties (e.g., stretchability, auxeticity, multistability, etc.) and mechanics of the nanomembrane. We then surveyed a versatile toolbox of actuation and fabrication strategies, ranging from capillary and residual-stress self-folding to magneto-electro-thermal reconfiguration, all of which leverage established planar lithography before inducing out-of-plane transformation. Three types of device applications are discussed. In optoelectronics, folded nanomembranes provide omnidirectional photodetection, strain-engineered band gaps, and dynamically tunable metasurfaces. In microrobotics, kirigami lattices, stress-programmed bilayers, and nanoscale magnetic encoders endow sub-millimeter machines with locomotion, gripping, and flight. In metamaterials, geometric hierarchies create mechanical modules with programmable stiffness or EM resonators whose spectra shift with each fold. Overall, these examples demonstrate four principle advantages of origami and kirigami on nanomembranes: i) scale-independent design that migrates seamlessly from millimetres to atomic layers; ii) materials compatibility with high-performance semiconductors, metals and polymers; iii) batch manufacturability via wafer-scale lithography followed by parallel folding; and iv) reconfigurability on demand, allowing a single device to deliver multiple, selectively addressable functions.

Origami and kirigami on nanomembranes can yield devices with unique capabilities compared to conventional designs. However, as an emerging technology, there remain significant challenges to address and exciting opportunities to pursue. Designing complex origami/kirigami patterns for specific functions is still largely a skilled craft or an iterative simulation process. The design space is huge (where to put creases/cuts, in what order they fold, etc.), and there are few automated tools. While progress is being made on origami design algorithms, it's a limitation that custom patterns often need to be invented for each new task. The issue of finite rigidity and material thickness is also a fundamental challenge. Although theoretical origami often assumes zero thickness, real nanomembranes have a finite thickness that can cause deviations from ideal folding behavior. Accommodating panel thickness in complex folds sometimes requires additional design tricks (e.g., offset hinges or extra folds). For intricate origami patterns, ensuring that the material doesn't self-intersect or lock up is a non-trivial design constraint, especially at microscale tolerances. Also, there is still a limited palette of proven nanomembrane materials that work well for folding. Silicon is popular but brittle; polymers are flexible but often not dimensionally stable or precise; metals can fatigue or creep. Emerging materials like 2D materials (graphene, MoS_2, etc.) with atomic thickness offer superb flexibility and strength, but large-area production of these at high quality is still maturing. Although many origami/kirigami devices have been made using batch processes, truly high-volume manufacturing (like wafer-scale CMOS) of complex foldable systems is still lacking. Additionally, some fabrication or actuation methods (like FIB-induced folding or manual transfer) are intrinsically low-throughput. Overcoming this may involve developing new self-folding materials that can be

activated. Actuation and control also demand progress. Thermal bimorphs and capillary folding are reliable but energy-intensive or single-shot; magneto-mechanical and electrostatic schemes promise reversible, low-power operation yet require complex control systems in laboratories. Each challenge also represents an opportunity for innovation that will drive the field into its next phase (**Figure 10**).

In conclusion, the future of origami and kirigami on nanomembranes is exceptionally bright and multidisciplinary. By overcoming current limitations and harnessing emerging technologies, we expect to see a new generation of smart, reconfigurable, and efficient microdevices. These systems might form the basis of programmable matter—materials that can change their physical properties or shape on command—a long-standing vision that now appears within reach. The convergence of innovations in materials (like 2D materials), microfabrication (like 3D lithography and printing), and computing (like AI-driven design and control) will accelerate progress. Ultimately, origami/kirigami nanomembrane techniques will likely transition from the lab to the real world in applications ranging from medicine to advanced optics, creating devices that are lighter, more compact, more versatile, and smarter. As next-generation multifunctional systems emerge, including self-folding robots, adaptive sensors, and tunable metamaterials, the folding of nanomembranes will be a key enabling technology.

Acknowledgements

This work is supported by the National Key Technologies R&D Program of China (Nos. 2022YFA1207000, 2022YFA1404700, and 2021YFA0715302), National Natural Science Foundation of China (Nos. 52101214, and 62375054), Shanghai Rising-Star Program (No. 24QA2700700), Science and Technology Commission of Shanghai Municipality (24520750200, 24CL2900200), and Shanghai Talent Programs.

Conflict of Interest

The authors have no conflicts to disclose.

Data Availability Statement

Data sharing is not applicable to this article as no new data were created or analyzed in this study.

Keywords

kirigami, microfabrication, Nanomembrane, origami

Received: June 9, 2025
Revised: August 21, 2025
Published online:

[1] R. J. Lang, *Origami Design Secrets: Mathematical Methods for an Ancient Art*, Second Edition, A K Peters/CRC Press, New York, NY **2011**.
[2] D. Misseroni, P. P. Pratapa, K. Liu, B. Kresling, Y. Chen, C. Daraio, G. H. Paulino, *Nat. Rev. Methods Primer* **2024**, *4*, 40.
[3] M. Meloni, J. Cai, Q. Zhang, D. Sang-Hoon Lee, M. Li, R. Ma, T. E. Parashkevov, J. Feng, *Adv. Sci.* **2021**, *8*, 2000636.
[4] L. Jin, S. Yang, *Adv. Mater.* **2024**, *36*, 2308560.
[5] J. A. Rogers, M. G. Lagally, R. G. Nuzzo, *Nature* **2011**, *477*, 45.
[6] Y. Zhang, Z. Yan, K. Nan, D. Xiao, Y. Liu, H. Luan, H. Fu, X. Wang, Q. Yang, J. Wang, W. Ren, H. Si, F. Liu, L. Yang, H. Li, J. Wang, X. Guo, H. Luo, L. Wang, Y. Huang, J. A. Rogers, *Proc. Natl. Acad. Sci* **2015**, *112*, 11757.
[7] G. Huang, Y. Mei, *Small* **2018**, *14*, 1703665.
[8] S. Chen, J. Chen, X. Zhang, Z.-Y. Li, J. Li, *Light Sci. Appl.* **2020**, *9*, 75.
[9] Z. Zhang, Z. Tian, Y. Mei, Z. Di, *Mater. Sci. Eng. R Rep.* **2021**, *145*, 100621.
[10] K. Zhang, Y. H. Jung, S. Mikael, J.-H. Seo, M. Kim, H. Mi, H. Zhou, Z. Xia, W. Zhou, S. Gong, Z. Ma, *Nat. Commun.* **2017**, *8*, 1782.
[11] Y. Mei, A. A. Solovev, S. Sanchez, O. G. Schmidt, *Chem. Soc. Rev.* **2011**, *40*, 2109.
[12] F. Gabler, D. D. Karnaushenko, D. Karnaushenko, O. G. Schmidt, *Nat. Commun.* **2019**, *10*, 3013.
[13] J. L. Silverberg, J.-H. Na, A. A. Evans, B. Liu, T. C. Hull, C. D. Santangelo, R. J. Lang, R. C. Hayward, I. Cohen, *Nat. Mater.* **2015**, *14*, 389.
[14] M. K. Blees, A. W. Barnard, P. A. Rose, S. P. Roberts, K. L. McGill, P. Y. Huang, A. R. Ruyack, J. W. Kevek, B. Kobrin, D. A. Muller, P. L. McEuen, *Nature* **2015**, *524*, 204.
[15] D. Jayachandran, N. U. Sakib, S. Das, *Nat. Rev. Electr. Eng.* **2024**, *1*, 300.
[16] G. Von Freymann, A. Ledermann, M. Thiel, I. Staude, S. Essig, K. Busch, M. Wegener, *Adv. Funct. Mater.* **2010**, *20*, 1038.
[17] M. Kadic, G. W. Milton, M. van Hecke, M. Wegener, *Nat. Rev. Phys.* **2019**, *1*, 198.
[18] A. Fernández-Pacheco, R. Streubel, O. Fruchart, R. Hertel, P. Fischer, R. P. Cowburn, *Nat. Commun.* **2017**, *8*, 15756.
[19] P. Jiao, J. Mueller, J. R. Raney, X. Zheng, A. H. Alavi, *Nat. Commun.* **2023**, *14*, 6004.
[20] Y. Wang, J. Liao, S. P. McBride, E. Efrati, X, L., H. M. Jaeger, *Nano Lett.* **2015**, *15*, 6732.
[21] X. Li, Y. Wang, B. Xu, X. Zhou, C. Men, Z. Tian, Y. Mei, *Nanotechnology* **2019**, *30*, 354003.
[22] Z. Liu, H. Du, J. Li, L. Lu, Z.-Y. Li, N. X. Fang, *Sci. Adv.* **2018**, *4*, aat4436.
[23] J. Cho, M. D. Keung, N. Verellen, L. L. Victor, V. Moshchalkov, P. V. Dorpe, D. H. Gracias, *Small* **2011**, *14*, 1943.
[24] B. Wu, Z. Zhang, Z. Zheng, T. Cai, C. You, C. Liu, X. Li, Y. Wang, J. Wang, H. Li, E. Song, J. Cui, G. Huang, Y. Mei, *Adv. Mater.* **2023**, *35*, 2306715.
[25] Z. Yan, F. Zhang, J. Wang, F. Liu, X. Guo, K. Nan, Q. Lin, M. Gao, D. Xiao, Y. Shi, Y. Qiu, H. Luan, J. H. Kim, Y. Wang, H. Luo, M. Han, Y. Huang, Y. Zhang, J. A. Rogers, *Adv. Funct. Mater.* **2016**, *26*, 2629.
[26] Y. M. Song, Y. Xie, V. Malyarchuk, J. Xiao, I. Jung, K.-J. Choi, Z. Liu, H. Park, C. Lu, R.-H. Kim, R. Li, K. B. Crozier, Y. Huang, J. A. Rogers, *Nature* **2013**, *497*, 95.
[27] Z. Liu, S. Du, A. Cui, Z. Li, Y. Fan, S. Chen, W. Li, J. Li, C. Gu, *Adv. Mater.* **2017**, *29*, 1606298.
[28] S. Chen, Z. Liu, H. Du, C. Tang, C.-Y. Ji, B. Quan, R. Pan, L. Yang, X. Li, C. Gu, X. Zhang, Y. Yao, J. Li, N. X. Fang, J. Li, *Nat. Commun.* **2021**, *12*, 1299.
[29] J. S. Randhawa, T. G. Leong, N. Bassik, B. R. Benson, M. T. Jochmans, D. H. Gracias, *J. Am. Chem. Soc.* **2008**, *130*, 17238.
[30] M. Z. Miskin, A. J. Cortese, K. Dorsey, E. P. Esposito, M. F. Reynolds, Q. Liu, M. Cao, D. A. Muller, P. L. McEuen, I. Cohen, *Nature* **2020**, *584*, 557.
[31] B. H. Kim, K. Li, J.-T. Kim, Y. Park, H. Jang, X. Wang, Z. Xie, S. M. Won, H.-J. Yoon, G. Lee, W. J. Jang, K. H. Lee, T. S. Chung, Y. H. Jung, S. Y. Heo, Y. Lee, J. Kim, T. Cai, Y. Kim, P. Prasopsukh, Y. Yu, X.

Yu, R. Avila, H. Luan, H. Song, F. Zhu, Y. Zhao, L. Chen, S. H. Han, J. Kim, et al., *Nature* **2021**, *597*, 503.
[32] J. Cui, T.-Y. Huang, Z. Luo, P. Testa, H. Gu, X.-Z. Chen, B. J. Nelson, L. J. Heyderman, *Nature* **2019**, *575*, 164.
[33] H. Wang, W. Zhang, D. Ladika, H. Yu, D. Gailevičius, H. Wang, C. Pan, P. N. S. Nair, Y. Ke, T. Mori, J. Y. E. Chan, Q. Ruan, M. Farsari, M. Malinauskas, S. Juodkazis, M. Gu, J. K. W. Yang, *Adv. Funct. Mater.* **2023**, *33*, 2214211.
[34] N. Zhang, Z. Wang, Z. Zhao, D. Zhang, J. Feng, L. Yu, Z. Lin, Q. Guo, J. Huang, J. Mao, J. Yang, *Microsyst. Nanoeng.* **2025**, *11*, 35.
[35] M. T. Tolley, S. M. Felton, S. Miyashita, D. Aukes, D. Rus, R. J. Wood, *Smart Mater. Struct.* **2014**, *23*, 094006.
[36] Y. Liu, B. Shaw, M. D. Dickey, J. Genzer, *Sci. Adv.* **2017**, *3*, 1602417.
[37] E. D. Demaine, J. O'Rourke, *Geometric Folding Algorithms: Linkages, Origami, Polyhedra*, Cambridge University Press, Cambridge, UK **2007**.
[38] J. O'Rourke, *How to Fold It: The Mathematics of Linkages, Origami, and Polyhedra*, Cambridge University Press, Cambridge, UK **2011**.
[39] M. Schenk, S. D. Guest, *Proc. Natl. Acad. Sci* **2013**, *110*, 3276.
[40] H. Nassar, A. Lebée, L. Monasse, *Proc. R. Soc. Math. Phys. Eng. Sci.* **2017**, *473*, 20160705.
[41] X. Dang, G. H. Paulino, *Proc. R. Soc. Math. Phys. Eng. Sci.* **2024**, *480*, 20230956.
[42] L. Lu, S. Leanza, R. R. Zhao, *Appl. Mech. Rev.* **2023**, *75*, 050801.
[43] S. P. Vasudevan, P. P. Pratapa, *J. Eng. Mech.* **2021**, *147*, 04021093.
[44] E. T. Filipov, T. Tachi, G. H. Paulino, *Proc. Natl. Acad. Sci* **2015**, *112*, 12321.
[45] Z. Zhai, Y. Wang, H. Jiang, *Proc. Natl. Acad. Sci* **2018**, *115*, 2032.
[46] J. L. Silverberg, A. A. Evans, L. McLeod, R. C. Hayward, T. Hull, C. D. Santangelo, I. Cohen, *Science* **2014**, *345*, 647.
[47] B. Liu, J. L. Silverberg, A. A. Evans, C. D. Santangelo, R. J. Lang, T. C. Hull, I. Cohen, *Nat. Phys.* **2018**, *14*, 811.
[48] L. Lu, S. Leanza, J. Dai, J. W. Hutchinson, R. R. Zhao, *Proc. Natl. Acad. Sci* **2024**, *121*, 2405744121.
[49] S. Xu, Z. Yan, K.-I. Jang, W. Huang, H. Fu, J. Kim, Z. Wei, M. Flavin, J. McCracken, R. Wang, A. Badea, Y. Liu, D. Xiao, G. Zhou, J. Lee, H. U. Chung, H. Cheng, W. Ren, A. Banks, X. Li, U. Paik, R. G. Nuzzo, Y. Huang, Y. Zhang, J. A. Rogers, *Science* **2015**, *347*, 154.
[50] G. W. Milton, *J. Mech. Phys. Solids* **2013**, *61*, 1543.
[51] Y. Tang, Y. Li, Y. Hong, S. Yang, J. Yin, *Proc. Natl. Acad. Sci* **2019**, *116*, 26407.
[52] X. Dang, S. Gonella, G. H. Paulino, *Proc. Natl. Acad. Sci* **2024**, *121*, 2413370121.
[53] P. M. Dodd, P. F. Damasceno, S. C. Glotzer, *Proc. Natl. Acad. Sci* **2018**, *115*, E6690.
[54] X. Dang, S. Chen, A. E. Acha, L. Wu, D. Pasini, *Sci. Adv.* **2025**, *11*, ads5659.
[55] P. Rajak, B. Wang, K. Nomura, Y. Luo, A. Nakano, R. Kalia, P. Vashishta, *Npj Comput. Mater.* **2021**, *7*, 102.
[56] X. Dang, F. Feng, P. Plucinsky, R. D. James, H. Duan, J. Wang, *Int. J. Solids Struct.* **2022**, *234*, 111224.
[57] K. Xiao, Z. Liang, B. Zou, X. Zhou, J. Ju, *Nat. Commun.* **2022**, *13*, 7474.
[58] C. Qiao, S. Chen, Y. Chen, Z. Zhou, W. Jiang, Q. Wang, X. Tian, D. Pasini, *Phys. Rev. Lett.* **2025**, *134*, 176103.
[59] Y. Zhu, M. Birla, K. R. Oldham, E. T. Filipov, *Adv. Funct. Mater.* **2020**, *30*, 2003741.
[60] Z. Song, C. Lv, M. Liang, V. Sanphuang, K. Wu, B. Chen, Z. Zhao, J. Bai, X. Wang, J. L. Volakis, L. Wang, X. He, Y. Yao, S. Tongay, H. Jiang, *Small* **2016**, *12*, 5401.
[61] Z. Rao, Y. Lu, Z. Li, K. Sim, Z. Ma, J. Xiao, C. Yu, *Nat. Electron.* **2021**, *4*, 513.
[62] E. Zhang, S. Ding, X. Li, X. Ma, X. Gao, L. Liu, Y. Shen, S. Cheng, W. Mi, Y. Zhou, G. Feng, Y. Song, X. Li, Y. Xue, K. Xin, X. Zeng, Q. Jiang, R. Zhang, X. Liu, Z. Wei, Q. Zeng, B. Wang, Q. Li, J. Liu, J. Yan, S. Lei, Y. Yang, W. Hu, *Nat. Mater.* **2025**, *24*, 377.
[63] Z. Zhang, Y. Wang, T. Cai, B. Wu, B. Hu, X. Li, E. Song, G. Huang, Z. Tian, Z. Di, Y. Mei, *Adv. Funct. Mater.* **2025**, *35*, 2502191.
[64] Y. Zong, M. Xi, Y. Wang, G. Zeng, D. Hu, H. Hu, X. Hou, K. Nan, X. Chen, F. Xu, O. G. Schmidt, Y. Mei, J. Cui, *Adv. Mater.* **2025**, *37*, 2418316.
[65] Q. Liu, W. Wang, H. Sinhmar, I. Griniasty, J. Z. Kim, J. T. Pelster, P. Chaudhari, M. F. Reynolds, M. C. Cao, D. A. Muller, A. B. Apsel, N. L. Abbott, H. Kress-Gazit, P. L. McEuen, I. Cohen, *Nat. Mater.* **2025**, *24*, 109.
[66] B. Zhao, Z. Wan, Y. Liu, J. Xu, X. Yang, D. Shen, Z. Zhang, C. Guo, Q. Qian, J. Li, R. Wu, Z. Lin, X. Yan, B. Li, Z. Zhang, H. Ma, B. Li, X. Chen, Y. Qiao, I. Shakir, Z. Almutairi, F. Wei, Y. Zhang, X. Pan, Y. Huang, Y. Ping, X. Duan, X. Duan, *Nature* **2021**, *591*, 385.
[67] D. H. Gracias, V. Kavthekar, J. C. Love, K. E. Paul, G. M. Whitesides, *Adv. Mater.* **2002**, *14*, 235.
[68] X. Guo, H. Li, B. Yeop Ahn, E. B. Duoss, K. J. Hsia, J. A. Lewis, R. G. Nuzzo, *Proc. Natl. Acad. Sci* **2009**, *106*, 20149.
[69] M. F. Reynolds, K. L. McGill, M. A. Wang, H. Gao, F. Mujid, K. Kang, J. Park, M. Z. Miskin, I. Cohen, P. L. McEuen, *Nano Lett.* **2019**, *19*, 6221.
[70] Z. Chen, G. Huang, I. Trase, X. Han, Y. Mei, *Phys. Rev. Appl.* **2016**, *5*, 017001.
[71] W. Huang, X. Yu, P. Froeter, R. Xu, P. Ferreira, X. Li, *Nano Lett.* **2012**, *12*, 6283.
[72] W. Huang, J. Zhou, P. J. Froeter, K. Walsh, S. Liu, M. D. Kraman, M. Li, J. A. Michaels, D. J. Sievers, S. Gong, X. Li, *Nat. Electron.* **2018**, *1*, 305.
[73] B. Wu, Z. Zhang, B. Chen, Z. Zheng, C. You, C. Liu, X. Li, J. Wang, Y. Wang, E. Song, J. Cui, Z. An, G. Huang, Y. Mei, *Sci. Adv.* **2023**, *9*, adi7805.
[74] Z. Zhang, T. Cai, Z. Li, B. Wu, Z. Zheng, C. You, G. Jiang, M. Ma, Z. Xu, C. Shen, X. Chen, E. Song, J. Cui, G. Huang, Y. Mei, *Adv. Mater.* **2025**, *37*, 2413771.
[75] Z. Tian, L. Zhang, Y. Fang, B. Xu, S. Tang, N. Hu, Z. An, Z. Chen, Y. Mei, *Adv. Mater.* **2017**, *29*, 1604572.
[76] X. Hong, B. Xu, G. Li, F. Nan, X. Wang, Q. Liang, W. Dong, W. Dong, H. Sun, Y. Zhang, C. Li, R. Fu, Z. Wang, G. Shen, Y. Wang, Y. Yao, S. Zhang, J. Li, *Sci. Adv.* **2024**, *10*, adn7582.
[77] R. Bo, S. Xu, Y. Yang, Y. Zhang, *Chem. Rev.* **2023**, *123*, 11137.
[78] M. Han, X. Guo, X. Chen, C. Liang, H. Zhao, Q. Zhang, W. Bai, F. Zhang, H. Wei, C. Wu, Q. Cui, S. Yao, B. Sun, Y. Yang, Q. Yang, Y. Ma, Z. Xue, J. W. Kwak, T. Jin, Q. Tu, E. Song, Z. Tian, Y. Mei, D. Fang, H. Zhang, Y. Huang, Y. Zhang, J. A. Rogers, *Sci. Robot.* **2022**, *7*, abn0602.
[79] W. J. Arora, H. I. Smith, G. Barbastathis, *Microelectron. Eng.* **2007**, *84*, 1454.
[80] X. Han, K. J. Seo, Y. Qiang, Z. Li, S. Vinnikova, Y. Zhong, X. Zhao, P. Hao, S. Wang, H. Fang, *Npj Flex. Electron.* **2019**, *3*, 9.
[81] Y. Mei, G. Huang, A. A. Solovev, E. B. Ureña, I. Mönch, F. Ding, T. Reindl, R. K. Y. Fu, P. K. Chu, O. G. Schmidt, *Adv. Mater.* **2008**, *20*, 4085.
[82] K. Malachowski, J. Breger, H. R. Kwag, M. O. Wang, J. P. Fisher, F. M. Selaru, D. H. Gracias, *Angew. Chem., Int. Ed.* **2014**, *53*, 8045.
[83] W. Wang, Q. Liu, I. Tanasijevic, M. F. Reynolds, A. J. Cortese, M. Z. Miskin, M. C. Cao, D. A. Muller, A. C. Molnar, E. Lauga, P. L. McEuen, I. Cohen, *Nature* **2022**, *605*, 681.
[84] Y. Wu, X. Zhang, Z. Ma, W. Hong, C. You, H. Zhu, Y. Zong, Y. Hu, B. Xu, G. Huang, Z. Di, Y. Mei, *ACS Nano* **2025**, *19*, 331.
[85] A. Carlson, A. M. Bowen, Y. Huang, R. G. Nuzzo, J. A. Rogers, *Adv. Mater.* **2012**, *24*, 5284.
[86] Z. Yan, M. Han, Y. Shi, A. Badea, Y. Yang, A. Kulkarni, E. Hanson, M. E. Kandel, X. Wen, F. Zhang, Y. Luo, Q. Lin, H. Zhang, X. Guo, Y.

Huang, K. Nan, S. Jia, A. W. Oraham, M. B. Mevis, J. Lim, X. Guo, M. Gao, W. Ryu, K. J. Yu, B. G. Nicolau, A. Petronico, S. S. Rubakhin, J. Lou, P. M. Ajayan, et al., *Proc. Natl. Acad. Sci* **2017**, *114*, E9455.
[87] R.-H. Kim, D.-H. Kim, J. Xiao, B. H. Kim, S.-I. Park, B. Panilaitis, R. Ghaffari, J. Yao, M. Li, Z. Liu, V. Malyarchuk, D. G. Kim, A.-P. Le, R. G. Nuzzo, D. L. Kaplan, F. G. Omenetto, Y. Huang, Z. Kang, J. A. Rogers, *Nat. Mater.* **2010**, *9*, 929.
[88] X. Hu, P. Krull, B. De Graff, K. Dowling, J. A. Rogers, W. J. Arora, *Adv. Mater.* **2011**, *23*, 2880.
[89] D. C. Kim, H. Yun, J. Kim, H. Seung, W. S. Yu, J. H. Koo, J. Yang, J. H. Kim, T. Hyeon, D.-H. Kim, *Nat. Electron.* **2021**, *4*, 671.
[90] L. Hu, J. Choi, S. Hwangbo, D.-H. Kwon, B. Jang, S. Ji, J.-H. Kim, S.-K. Han, J.-H. Ahn, *Npj Flex. Electron.* **2022**, *6*, 100.
[91] R. Su, S. H. Park, X. Ouyang, S. I. Ahn, M. C. McAlpine, *Sci. Adv.* **2022**, *8*, abl8798.
[92] W. Lee, Y. Liu, Y. Lee, B. K. Sharma, S. M. Shinde, S. D. Kim, K. Nan, Z. Yan, M. Han, Y. Huang, Y. Zhang, J.-H. Ahn, J. A. Rogers, *Nat. Commun.* **2018**, *9*, 1417.
[93] C.h. Strelow, C. M. Schultz, H. Rehberg, M. Sauer, H. Welsch, A. Stemmann, C.h. Heyn, D. Heitmann, T. Kipp, *Phys. Rev. B* **2012**, *85*, 155329.
[94] X. Wang, Z. Wang, H. Dong, C. N. Saggau, H. Tang, M. Tang, L. Liu, S. Baunack, L. Bai, J. Liu, Y. Yin, L. Ma, O. G. Schmidt, *Nano Lett.* **2022**, *22*, 6692.
[95] H. Wang, H. Zhen, S. Li, Y. Jing, G. Huang, Y. Mei, W. Lu, *Sci. Adv.* **2016**, *2*, 1600027.
[96] H. Li, A. W. Contryman, X. Qian, S. M. Ardakani, Y. Gong, X. Wang, J. M. Weisse, C. H. Lee, J. Zhao, P. M. Ajayan, J. Li, H. C. Manoharan, X. Zheng, *Nat. Commun.* **2015**, *6*, 7381.
[97] H. Chen, X.-L. Zhang, Y.-Y. Zhang, D. Wang, D.-L. Bao, Y. Que, W. Xiao, S. Du, M. Ouyang, S. T. Pantelides, H.-J. Gao, *Science* **2019**, *365*, 1036.
[98] H. Zhou, S. Zhang, Z. Liu, B. Chi, J. Li, Y. Wang, *Small* **2024**, *20*, 2305805.
[99] T. G. Leong, C. L. Randall, B. R. Benson, N. Bassik, G. M. Stern, D. H. Gracias, *Proc. Natl. Acad. Sci* **2009**, *106*, 703.
[100] K. Malachowski, M. Jamal, Q. Jin, B. Polat, C. J. Morris, D. H. Gracias, *Nano Lett.* **2014**, *14*, 4164.
[101] J. C. Breger, C. Yoon, R. Xiao, H. R. Kwag, M. O. Wang, J. P. Fisher, T. D. Nguyen, D. H. Gracias, *ACS Appl. Mater. Interfaces* **2015**, *7*, 3398.
[102] Q. Jin, Y. Yang, J. A. Jackson, C. Yoon, D. H. Gracias, *Nano Lett.* **2020**, *20*, 5383.
[103] K. Kobayashi, C. Yoon, S. H. Oh, J. V. Pagaduan, D. H. Gracias, *ACS Appl. Mater. Interfaces* **2019**, *11*, 151.
[104] H. Xu, S. Wu, Y. Liu, X. Wang, A. K. Efremov, L. Wang, J. S. McCaskill, M. Medina-Sánchez, O. G. Schmidt, *Nat. Nanotechnol.* **2024**, *19*, 494.
[105] L. Zhang, J. J. Abbott, L. Dong, B. E. Kratochvil, D. Bell, B. J. Nelson, *Appl. Phys. Lett.* **2009**, *94*, 064107.
[106] C. L. Smart, T. G. Pearson, Z. Liang, M. X. Lim, M. I. Abdelrahman, F. Monticone, I. Cohen, P. L. McEuen, *Science* **2024**, *386*, 1031.
[107] Y. Chen, C. Valenzuela, X. Zhang, X. Yang, L. Wang, W. Feng, *Nat. Commun.* **2023**, *14*, 3036.
[108] H.-J. Yoon, G. Lee, J.-T. Kim, J.-Y. Yoo, H. Luan, S. Cheng, S. Kang, H. L. T. Huynh, H. Kim, J. Park, J. Kim, S. S. Kwak, H. Ryu, J. Kim, Y. S. Choi, H.-Y. Ahn, J. Choi, S. Oh, Y. H. Jung, M. Park, W. Bai, Y. Huang, L. P. Chamorro, Y. Park, J. A. Rogers, *Sci. Adv.* **2022**, *8*, ade3201.
[109] J.-T. Kim, H.-J. Yoon, S. Cheng, F. Liu, S. Kang, S. Paudel, D. Cho, H. Luan, M. Lee, G. Jeong, J. Park, Y.-T. Huang, S. E. Lee, M. Cho, G. Lee, M. Han, B. H. Kim, J. Yan, Y. Park, S. Jung, L. P. Chamorro, J. A. Rogers, *PNAS Nexus* **2024**, *3*, 110.
[110] Z. Guo, B. Ji, L. Wang, B. Yang, W. Wang, J. Liu, 2020 IEEE 33rd International Conference on Micro Electro Mechanical Systems (MEMS), Vancouver, BC, Canada, **2020**, pp. 350–353.
[111] X. Yang, C. Forro, T. L. Li, Y. Miura, T. J. Zaluska, C. Tsai, S. Kanton, J. P. McQueen, X. Chen, V. Mollo, F. Santoro, S. P. Pasca, B. Cui, *Nat. Biotechnol.* **2024**, *42*, 1836.
[112] L. Coles, D. Ventrella, A. Carnicer-Lombarte, A. Elmi, J. G. Troughton, M. Mariello, S. E. Hadwe, B. J. Woodington, M. L. Bacci, G. G. Malliaras, D. G. Barone, C. M. Proctor, *Nat. Commun.* **2024**, *15*, 6290.
[113] Y. Gong, X. Liu, Z. Jiang, A. Weber, W. Li, *Microsyst. Nanoeng.* **2025**, *11*, 76.
[114] M. Jung, J. A. Shihada, S. Decke, L. Koschinski, P. S. Graff, S. M. Pazmino, A. Höllig, H. Koch, S. Musall, A. Offenhäusser, V. R. Montes, *Adv. Mater.* **2025**, *37*, 2418524.
[115] Z. Lin, L. S. Novelino, H. Wei, N. A. Alderete, G. H. Paulino, H. D. Espinosa, S. Krishnaswamy, *Small* **2020**, *16*, 2002229.
[116] Z. Tian, B. Xu, G. Wan, X. Han, Z. Di, Z. Chen, Y. Mei, *Nat. Commun.* **2021**, *12*, 509.
[117] M. Zhang, H. Shahsavan, Y. Guo, A. Pena-Francesch, Y. Zhang, M. Sitti, *Adv. Mater.* **2021**, *33*, 2008605.
[118] P. Shi, Y. Chen, J. Feng, P. Sareh, *Phys. Rev. E* **2024**, *109*, 035002.
[119] Z. Liu, H. Du, Z. Li, N. X. Fang, J. Li, *APL Photonics* **2018**, *3*, 100803.
[120] Y. Han, S. Chen, C. Ji, X. Liu, Y. Wang, J. Liu, J. Li, *Opt. Express* **2021**, *29*, 30751.
[121] Z. Liu, Y. Xu, C. Ji, S. Chen, X. Li, X. Zhang, Y. Yao, J. Li, *Adv. Mater.* **2020**, *32*, 1907077.
[122] H. Tao, A. C. Strikwerda, K. Fan, W. J. Padilla, X. Zhang, R. D. Averitt, *Phys. Rev. Lett.* **2009**, *103*, 147401.
[123] Q. Liang, Z. Liu, Y. Han, S. Chen, H. Sun, Y. Chen, Y. Zhang, M. Niu, C. Li, Y. Wang, K. Jin, Y. Wang, Y. Yao, J. Liu, J. Li, *Nat. Commun.* **2025**, *16*, 5512.

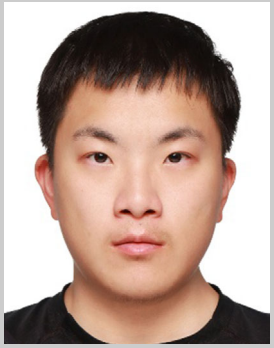

Xiang Dong is currently a Ph.D. candidate in the College of Intelligent Robotics and Advanced Manufacturing at Fudan University. He received his B.A. degree in physics from the University of Colorado Boulder and his M.S. degree in electrical and computer engineering from the University of California, Los Angeles. His research interests focus on materials epitaxy growth and nanomembrane 3D structures.

Xing Li is a postdoctoral fellow in the College of Intelligent Robotics and Advanced Manufacturing, Fudan University. Prior to that, he received his B.S. and M.S. degrees from the University of Shanghai for Science and Technology in 2016 and 2019, and a Ph.D. degree in microelectronics and solid state electronics from Fudan University in 2023. His research interests include deposition of smart material nanomembranes and fabrication of three-dimensional electronic devices.

Jizhai Cui is a tenure-track associate professor at the International Institute for Intelligent Nanorobots and Nanosystems, College of Intelligent Robotics and Advanced Manufacturing, Fudan University. He obtained his Ph.D. in mechanical engineering from the University of California, Los Angeles, in 2016 and subsequently held postdoctoral appointments in the Department of Materials at ETH Zurich and the Paul Scherrer Institute. His research interests include intelligent micro- and nanorobots, origami/kirigami-inspired metamaterials, and nanomagnetic devices.

Yongfeng Mei is a professor at the International Institute for Intelligent Nanorobots and Nanosystems, College of Intelligent Robotics and Advanced Manufacturing, Fudan University, Shanghai. He received his B.S. and M.S. degrees in physics from Nanjing University and a Ph.D. in materials physics from City University of Hong Kong. He subsequently conducted postdoctoral research at the Max Planck Institute for Solid State Research and later led a research group as a staff scientist at the Leibniz Institute for Solid State and Materials Research Dresden. His current research centers on inorganic nanomembranes and their optical, optoelectronic, flexible electronic, and micro/nanorobotic applications.